

Data-Driven Kalman Filter using Maximum Likelihood Optimization [★]

Peihu Duan ^a, Tao Liu ^b, Yu Xing ^a, Karl Henrik Johansson ^a

^a*School of Electrical Engineering and Computer Science, KTH Royal Institute of Technology, Stockholm, Sweden*

^b*Department of Electrical and Electronic Engineering, The University of Hong Kong, Hong Kong SAR, China*

Abstract

This paper investigates the state estimation problem for unknown linear systems with process and measurement noise. A novel data-driven Kalman filter (DDKF) that combines model identification with state estimation is developed using pre-collected input-output data and uncertain initial state information of the unknown system. Specifically, the state estimation problem is first formulated as a non-convex maximum likelihood (ML) optimization problem. Then, to reduce the computational complexity, the optimization problem is broken down into a series of sub-problems in a recursive manner. Based on the optimal solutions to the sub-problems, a closed-form DDKF is designed for the unknown system, which can estimate the state of a physically meaningful state-space realization, rather than these up to an unknown similarity transformation. The performance gap between the DDKF and the traditional Kalman filter with accurate system matrices is quantified through a sample complexity bound. In particular, when the number of the pre-collected trajectories tends to infinity, this gap converges to zero. Moreover, the DDKF is used to facilitate data-driven control design. A data-driven linear quadratic Gaussian controller is defined and its closed-loop performance is characterized. Finally, the effectiveness of the theoretical results is illustrated by numerical simulations.

Key words: Kalman filter, Maximum likelihood, Data-driven filter, Sample complexity

1 Introduction

Due to its ability to estimate the state of dynamic systems, Kalman filtering has attracted tremendous attention since its inception in 1960 [1]. It has also been extensively applied in practice, such as aircraft navigation in aerospace [2], medical image reconstruction in medicine [3], and environmental monitoring in biology [4]. However, the effectiveness of Kalman filters is highly dependent on the prior knowledge of the precise structure and parameters of system dynamics that may be unavailable in some practical implementations [5]. To tackle this issue, research efforts have been devoted to system identification using pre-collected system data, considered as

preliminary for the filter design [6].

Motivated by the recent remarkable development of artificial intelligence, learning Kalman filters directly from data has become a hot research tendency [7]. Nevertheless, many vital issues in the design of data-driven Kalman filters (DDKFs) remain open. The main challenges include 1) how to excavate the underlying system dynamics from pre-collected noisy data for the filter design; 2) how to incorporate the performance analysis into the DDKF synthesis; 3) how to preserve the advantages, such as optimality and low complexity, of the model-based Kalman filter in DDKFs. This paper will concentrate on solving these tricky challenges.

1.1 Relevant Results

Learning from data has been a longstanding topic in the control society and is frequently utilized for the controller design [8]. The pioneering idea can be traced back to adaptive control [9]. Later, reinforcement learning developed in computer science provides a solid foundation for system dynamics representation and control strategy design using neural networks [10]. However, this

[★] This work was partially supported by Swedish Research Council Distinguished Professor Grant 2017-01078 and a Knut and Alice Wallenberg Foundation Wallenberg Scholar Grant.

^{**}P. Duan, Y. Xing, and K.H. Johansson are also affiliated with Digital Futures, Stockholm, Sweden.

Email addresses: peihu@kth.se (Peihu Duan), taoliu@eee.hku.hk (Tao Liu), yuxing2@kth.se (Yu Xing), kallej@kth.se (Karl Henrik Johansson).

method is resource-consuming and hard to interpret. Another effective tool to deal with unknown system dynamics is the Koopman operator, which describes the evolution of measurements in an infinite dimensional Hilbert space [11], but it is sensitive to the system noise. Recently, Willems’ fundamental lemma established in the behavioral theory contributes to several essential results on direct data-driven control [12–16]. These results mainly build on noise-free or noise-bounded data. In addition, some well-developed identification methods have been adopted for learning from data mingled with random noise [17–20], where a “system identification + robust control” scheme is usually used. For example, a so-called “Coarse-ID control” strategy for linear quadratic regulator (LQR) problem using pre-collected system input-state data was proposed to ensure an end-to-end sample-complexity control performance in [18]. Zheng et al. [20] generalized this result to linear quadratic Gaussian (LQG) control.

Inspired by the tremendous success of data-driven control and nourished by similar mathematical technologies, learning Kalman filters from data is starting to flourish [21–28]. An adaptive Kalman filter [21] and a distributionally robust Kalman filter [22] were proposed for systems with unknown noise covariance matrices. A “subspace system identification + certainty equivalent filtering” architecture only using output data was introduced for unknown linear systems in [23, 24], where the state can be estimated up to an unknown similarity transformation. A hybrid data-driven/model-based filter was developed using neural networks in [25, 26]. A Koopman operator-theoretic data-driven filter was designed in [27]. In [28], a missing data approach to data-driven filter design was proposed for systems under a kernel representation. In addition, some advanced data-driven parameter estimation approaches evolved from machine learning have been developed [29–31], which are more effective for constant parameters than dynamic variables.

1.2 Motivations

Despite the dual relationship between the control and filtering problems, it is not always practical to apply the existing data-driven control technologies directly to solve state estimation issues. For instance, the Willems’ fundamental lemma-based control technologies using input-output data may be infeasible for the filter design [12–20]. The main obstacle is that, for most control tasks, any state-space realization of the system is sufficient. However, when it comes to state estimation, especially for monitoring purposes, it becomes essential to pinpoint the specific state-space realization that characterizes the system state with physical meaning [32]. A practical example is given below to emphasize the significance of state estimation for such a realization.

Example 1: In most DC motor applications, monitoring

the rotational velocity is an essential issue [33]. Franklin et al. [34] presented a state-space realization for the dynamics of DC motor systems, given by:

$$\begin{bmatrix} \ddot{\theta} \\ \dot{i} \end{bmatrix} = \begin{bmatrix} -\frac{b}{J} & \frac{K_t}{J} \\ -\frac{K_e}{L_a} & -\frac{R_a}{L_a} \end{bmatrix} \begin{bmatrix} \dot{\theta} \\ i \end{bmatrix} + \begin{bmatrix} -\frac{T_L}{J} \\ \frac{V_a}{L_a} \end{bmatrix},$$

where $\dot{\theta}$, i , T_L , and V_a represent the rotational velocity, current, load torque, and DC voltage input, respectively, and b , K_t , J , K_e , R_a , and L_a are motor parameters. Let $x = [\dot{\theta}, i]^T$, $u = [T_L, V_a]^T$, and $y = i$ be the system state, input, and output, respectively. In the given state-space realization, the state variable x holds physical meaning, unlike states in realizations up to an unknown similarity transformation. Hence, it is crucial to prioritize state estimation for this particular realization for monitoring the rotational velocity. Identifying such a realization requires the incorporation of additional system knowledge along with input-output data [32]. This paper studies data-driven state estimation for such a physical realization, which is identified using both uncertain initial state information and noisy input-output data collected from past system trajectories.

In addition, the conventional data-driven filtering techniques may have various limitations for practical applications. Specifically, the neural network-based filtering methods may require huge amounts of computational resources and data to train the system model. Even with an identified model, the black-box nature makes the quantitative filtering performance analysis difficult. The Koopman operator-based methods are also restricted by similar issues. Besides, the lifting mapping mechanism embedded in the Koopman operator renders this strategy vulnerable to noise. The existing subspace identification-based filtering methods mainly conduct state estimation for a state-space realization up to an unknown similarity transformation, rather than the one with physical meaning.

Altogether, the challenges of integrating existing learning techniques from control into filtering and the limitations of traditional data-driven filtering methods suggest that the DDKF design problem remains open.

1.3 Contributions

This paper aims to develop a systematic data-driven filtering architecture for unknown linear systems affected by both process and measurement noise. The filtering performance and the computational efficiency of the architecture need to be ensured simultaneously. To achieve this target, this paper proposes a novel DDKF using the maximum likelihood (ML) principle and multiple previous system trajectories. Compared with existing results, this paper has four main advantages as follows.

- (1) The state estimation problem for unknown linear systems is formulated as an ML-based optimization problem using pre-collected system data. By solving this problem, the state estimates are directly obtained. Different from Willems' fundamental lemma-based methods that are more applicable to cases with bounded measurement noise [12–15], the proposed method is able to deal with both random process and measurement noise.
- (2) A computation-efficient method is proposed for solving the ML-based optimization problem. Its closed-form solution creates a novel recursive DDKF (**Algorithm 1**), which has much lower complexity than the neural network or Koopman operator-based state estimation methods [25–27]. Moreover, by incorporating the initial state information in the pre-collected data, a state estimate sequence can be determined for the exact realization of physical meaning, rather than the ones up to an unknown similarity transformation [23, 24].
- (3) The filtering performance of the designed DDKF is guaranteed (**Theorem 1**). In particular, a sample-complexity bound is derived for the performance gap between the DDKF and the traditional Kalman filter with accurate system matrices.
- (4) Based on the proposed DDKF, both static and dynamic data-driven output feedback controllers are proposed (**Theorems 2 and 3**). Further, by integrating the dynamic controller with the DDKF, a novel data-driven LQG control approach is developed with an end-to-end performance guarantee.

1.4 Organization

The remainder of this paper is organized as follows. Section 2 gives the problem formulation. Section 3 proposes a novel DDKF framework. Section 4 analyzes the necessary informativity of the pre-collected data required for performing the proposed DDKF. Section 5 evaluates the filtering performance of the DDKF. Based on the designed filtering framework, two types of data-driven output feedback controllers are developed in Section 6. The obtained theoretical results are illustrated by numerical examples in Section 7. Section 8 concludes the paper.

Notations: Let \mathbb{R}^n denote the real coordinate space of dimension n . Let \otimes denote the Kronecker product. Let I_n denote the n -order identity matrix. Let 0 denote a scalar, vector, or matrix of an appropriate dimension with all elements being zero. Let \mathbb{N}^+ be the set of positive integers and $\mathbb{N} = \mathbb{N}^+ \cup 0$. For any given vector μ and positive definite matrix Σ with appropriate dimensions, let $\mathcal{N}(\mu, \Sigma)$ denote Gaussian distribution with mean μ and covariance Σ . For a sequence of data s_1, \dots, s_N , let $\{s_t\}_{t=1}^N$ denote the set $\{s_1, \dots, s_N\}$. For any positive function f , let $\ln f$ denote its natural logarithm. For any matrix S , $S(m_1 : m_2; n_1 : n_2)$ denotes the block matrix in S with elements S_{ij} , $m_1 \leq i \leq m_2$, $n_1 \leq j \leq n_2$; S^\dagger

denotes its right/left inverse if it has full row/column rank. For a square matrix S , $|S|$ denotes its determinant; $\lambda(S)$ denotes the set of its eigenvalues; $\lambda_{\max}(S)/\lambda_{\min}(S)$ denotes its maximum/minimum eigenvalue if it is positive definite; and $S > 0$ ($S \geq 0$) denotes S is positive definite (semi-definite).

2 Problem Formulation

2.1 Preliminaries

This paper considers a class of linear time-invariant systems, whose dynamics are described by

$$\begin{aligned} x_{k+1} &= Ax_k + Bu_k + \omega_k, \\ y_k &= Cx_k + \nu_k, \quad k \in \mathbb{N}, \end{aligned} \quad (1)$$

where $x_k \in \mathbb{R}^n$, $u_k \in \mathbb{R}^m$, and $y_k \in \mathbb{R}^p$ denote the system state, input, and measurement at time step k , respectively; $A \in \mathbb{R}^{n \times n}$, $B \in \mathbb{R}^{n \times m}$, and $C \in \mathbb{R}^{p \times n}$ are the system state, input, and output matrices, respectively; $\omega_k \in \mathbb{R}^n \sim \mathcal{N}(0, Q)$ and $\nu_k \in \mathbb{R}^p \sim \mathcal{N}(0, R)$ are the system process and measurement noise with $Q \in \mathbb{R}^{n \times n} > 0$ and $R \in \mathbb{R}^{p \times p} > 0$, respectively. The initial system state is denoted by $x_0 \sim \mathcal{N}(\bar{x}_0, P_0)$ with $\bar{x}_0 \in \mathbb{R}^n$ and $P_0 \in \mathbb{R}^{n \times n} > 0$. In this paper, the system matrices A , B , and C in (1) are unknown. We assume that x_0 , ω_k , and ν_k , $\forall k \in \mathbb{N}$, are mutually uncorrelated.

Assumption 1 (C, A) is observable.

To estimate the state of system (1) with known A, B , and C , Kalman filtering is an effective method. Specifically, we denote the system inputs and outputs of one online observed trajectory by

$$\begin{aligned} u &= [u_0^T, u_1^T, \dots, u_k^T]^T, \\ y &= [y_1^T, y_2^T, \dots, y_{k+1}^T]^T. \end{aligned} \quad (2)$$

The *a posteriori* MMSE estimate of the system state at time step $k+1$, $k \in \mathbb{N}$, is defined as

$$\hat{x}_{k+1} = \mathbb{E}\{x_{k+1}|u, y\}. \quad (3)$$

According to [5], we can use the following Kalman filter to generate the value of \hat{x}_{k+1}

$$\hat{x}_{k+1|k} = A\hat{x}_k + Bu_k, \quad (4a)$$

$$\hat{x}_{k+1} = \hat{x}_{k+1|k} + L_{k+1}(y_{k+1} - C\hat{x}_{k+1|k}), \quad (4b)$$

$$L_{k+1} = \bar{P}_{k+1}C^T(R + C\bar{P}_{k+1}C^T)^{-1}, \quad (4c)$$

$$\bar{P}_{k+1} = AP_kA^T + Q, \quad (4d)$$

$$P_{k+1} = \bar{P}_{k+1} - \bar{P}_{k+1}C^T(R + C\bar{P}_{k+1}C^T)^{-1}C\bar{P}_{k+1}. \quad (4e)$$

where $\hat{x}_{k+1|k}$ is the *a priori* MMSE estimate, and L_{k+1} , \bar{P}_{k+1} and P_{k+1} are recursive filter matrices. The above

Kalman filter can also be derived using ML optimization [35]. Let $\hat{x} \triangleq [\hat{x}_0^T, \hat{x}_1^T, \dots, \hat{x}_{k+1}^T]^T$ be the augmented form of state estimates, and \mathbf{y} and \mathbf{x} be the associated random variables of y and \hat{x} , respectively. Then, the joint probability density function of the system states and outputs can be derived as [36, Lemma 9.6.1]

$$\begin{aligned} & f_{\mathbf{x}, \mathbf{y}}(\mathbf{x} = \hat{x}, \mathbf{y} = y) \\ &= f_{\text{con}} \times \exp\left(-\frac{1}{2} \sum_{t=0}^k \hat{\omega}_t^T Q^{-1} \hat{\omega}_t - \frac{1}{2} \sum_{t=0}^k \hat{\nu}_{t+1}^T R^{-1} \hat{\nu}_{t+1}\right. \\ &\quad \left. - \frac{1}{2} (\hat{x}_0 - \bar{x}_0)^T P_0^{-1} (\hat{x}_0 - \bar{x}_0)\right), \\ &\triangleq f(\hat{x}_0, \hat{\omega}, \hat{\nu} | u, y) \end{aligned}$$

where \hat{x}_0 is the estimate of x_0 , $\hat{\omega} \triangleq [\hat{\omega}_0^T, \dots, \hat{\omega}_k^T]^T$ and $\hat{\nu} \triangleq [\hat{\nu}_1^T, \dots, \hat{\nu}_{k+1}^T]^T$ are variables to model the system process and measurement noise respectively, with elements $\hat{\omega}_t$ and $\hat{\nu}_t$ satisfying

$$\begin{aligned} \hat{x}_{t+1} &= A\hat{x}_t + Bu_t + \hat{\omega}_t, \\ y_t &= C\hat{x}_t + \hat{\nu}_t, \quad t = 0, 1, \dots, k+1, \end{aligned} \quad (5)$$

and f_{con} is a constant. According to [36, Lemma 9.6.1], the optimal solution of variable \hat{x} to the optimization problem (6) corresponds to the *a posteriori* MMSE estimate defined in (3).

$$\begin{aligned} & \underset{\hat{x}_0, \hat{\omega}, \hat{\nu}}{\text{minimize}} && -f(\hat{x}_0, \hat{\omega}, \hat{\nu} | u, y) \\ & \text{s.t.} && (5). \end{aligned} \quad (6)$$

This indicates that Kalman filters can be inferred using ML optimization when A , B , and C are known.

2.2 Data Collection

Suppose that we have collected a set of input-output data of system (1) by conducting N mutually independent experiments, which will be used for data-driven state estimation for system (1) as formulated in Section 2.3. In the i -th experiment, we set the input sequence $\{u_h^i\}_{h=0}^{L-1}$ for (1) and collect the corresponding output sequence $\{y_h^i\}_{h=0}^L$, where $i \in \mathcal{V} \triangleq \{1, \dots, N\}$ and L is the sequence length. The data of the i -th input-output trajectory is denoted by

$$\begin{aligned} u^{i, \text{p}} &= [(u_0^i)^T, \dots, (u_{L-1}^i)^T]^T, \\ y^{i, \text{p}} &= [(y_0^i)^T, \dots, (y_L^i)^T]^T, \end{aligned}$$

where the superscript ‘p’ denotes the pre-collected data. Then, the augmented input and output data embodying all trajectories are denoted by

$$\begin{aligned} u^{\text{p}} &= [(u^{1, \text{p}})^T, \dots, (u^{N, \text{p}})^T]^T, \\ y^{\text{p}} &= [(y^{1, \text{p}})^T, \dots, (y^{N, \text{p}})^T]^T, \end{aligned} \quad (7)$$

respectively. In the i -th experiment, we assume that the initial state x_0^i is unknown, but its mean \bar{x}_0^i is known. Since the initial state x_0^i satisfies the Gaussian distribution, i.e., $x_0^i \sim \mathcal{N}(\bar{x}_0^i, P_0)$, $\forall i \in \mathcal{V}$, x_0^i can be rewritten as $x_0^i = \bar{x}_0^i + \xi^i$ where $\xi^i \sim \mathcal{N}(0, P_\xi)$ with $P_\xi = P_0$. Based on (1), we have

$$y_0^i = Cx_0^i + \nu_0^i, \quad \forall i \in \mathcal{V}, \quad (8)$$

and

$$\begin{aligned} y_h^i &= Cx_h^i + \nu_h^i \\ &= C(Ax_{h-1}^i + Bu_{h-1}^i + \omega_{h-1}^i) + \nu_h^i \\ &\quad \vdots \\ &= CA^h(\bar{x}_0^i + \xi_i) + \nu_h^i + \sum_{l=1}^h CA^{l-1}(Bu_{h-l}^i + \omega_{h-l}^i), \end{aligned} \quad (9)$$

for all $h \in \{1, \dots, L\}$ and $i \in \mathcal{V}$. Let $\omega^{i, \text{p}}$ and $\nu^{i, \text{p}}$ defined below be the corresponding unknown process and measurement noise, respectively,

$$\begin{aligned} \omega^{i, \text{p}} &= [(\omega_0^i)^T, \dots, (\omega_{L-1}^i)^T]^T, \\ \nu^{i, \text{p}} &= [(\nu_0^i)^T, \dots, (\nu_L^i)^T]^T. \end{aligned}$$

Further, we define the following notations

$$\begin{aligned} U &= [u^{1, \text{p}}, \dots, u^{N, \text{p}}], & Y &= [y^{1, \text{p}}, \dots, y^{N, \text{p}}], \\ \Omega &= [\omega^{1, \text{p}}, \dots, \omega^{N, \text{p}}], & V &= [\nu^{1, \text{p}}, \dots, \nu^{N, \text{p}}], \\ \bar{X}_0 &= [\bar{x}_0^1, \dots, \bar{x}_0^N], & \Xi &= [\xi^1, \dots, \xi^N]. \end{aligned} \quad (10)$$

Then, (8) and (9) can be rewritten in a matrix form as

$$Y = G\bar{X}_0 + H(I_L \otimes B)U + G\Xi + H\Omega + V, \quad (11)$$

where

$$G = [C^T, (CA)^T, \dots, (CA^L)^T]^T,$$

and

$$H = \begin{bmatrix} 0 & 0 & 0 & 0 \\ C & 0 & 0 & 0 \\ CA & C & 0 & 0 \\ \vdots & & \ddots & \vdots \\ CA^{L-1} & CA^{L-2} & \dots & C \end{bmatrix}.$$

Two assumptions on the pre-collected data are made.

Assumption 2 $L \geq n$.

Assumption 3 $\text{rank} \begin{bmatrix} \bar{X}_0 \\ U \end{bmatrix} = n + Lm$.

Assumption 2 is used to ensure the observability matrix $G(1 : Lp; 1 : n)$ defined below (11) has full column rank [37, Theorem 6.DO1]. Assumption 3 is a persistent excitation condition similar to these in system identification and Willems' fundamental lemma-based data-driven control [13, 17], which usually holds for a sufficiently large N . A slight difference between them is that Assumption 3 additionally requires the initial state information in order to determine the exact state-space realization of physical meaning rather than these up to a transformation similarity.

2.3 Problem Statement

This paper considers a system having a physically meaningful realization (1), yet the matrices A , B , and C are unknown. The objective of this paper is to estimate the state associated with the input-output trajectory (2) for this system. It is required that the state estimates should match the exact state-space realization (1) with the specific matrices A , B , and C , rather than these up to a similarity transformation, such as a balanced realization. As discussed in Section 1.2, these estimates not only help with control but also with monitoring applications. To achieve this goal, we have the knowledge of 1) the input-output data u^p and y^p of previous trajectories, and the associated means of initial states \bar{X}_0 , defined in (7) and (10), respectively; 2) the input-output data u and y of the observed trajectory defined in (2). Now, we describe the problem in a mathematical form as follows.

Problem: For system (1) with unknown A , B , and C , design a filtering framework to estimate the state corresponding to the input-output trajectory u and y defined in (2), by leveraging the pre-collected system data u^p , y^p , and \bar{X}_0 , as

$$\hat{x}_k = g(u, y, u^p, y^p, \bar{X}_0), \quad k \in \mathbb{N},$$

where $g(\cdot)$ denotes the framework, and \hat{x}_k represents the estimate of the state at step k that corresponds to the specific state-space realization described by (1). Moreover, the performance of the designed framework should be quantitatively analyzed and compared with the traditional Kalman filter with accurate system matrices (4).

The primary difficulty in solving the above problem is the handling of multi-source stochastic noise. The pre-collected offline data embody both process and measurement noise, and the online observed trajectory is also affected by random noise. The multi-source noise may result in ill-conditioned filters using existing data-driven theories. Another challenge is the need to determine the particular state-space realization described by (1) with the specific matrices A , B , and C . This requirement differs from the data-based estimation in the fields of sub-space identification, where the state is estimated up to an unknown similarity transformation using input-output

data [32]. To fulfill this requirement, we will leverage the initial state information in the pre-collected system trajectories.

3 DDKF Design

In this section, a novel data-driven filtering framework using ML optimization is proposed. The filtering problem is first formulated as a non-convex optimization problem, whose optimal solution is regarded as the state estimate. Subsequently, a computation-friendly approach is proposed to solve this problem, enabling state estimation to be performed recursively. This approach is referred to as a DDKF, specified in Algorithm 1.

3.1 ML-Based Data-Driven Filter

This subsection is aimed at providing a novel approach to estimating the system state of the online trajectory (2) using the input-output data u^p and y^p of previous trajectories, and the associated means of initial states \bar{X}_0 , defined in (7) and (10), respectively.

Before moving on, let \mathbf{y}^p be the random variable of the pre-collected output y^p defined in (7), and recall the definitions of \mathbf{x} and \mathbf{y} below (4). Motivated by the argument in Section 2.1, we define a joint probability density function of the system states and outputs of the online observed trajectory (2), and the initial states and outputs of previous trajectories (7), as

$$f_{\mathbf{x}, \mathbf{y}, \mathbf{y}^p}(\hat{x}, y, y^p) \triangleq f_{\mathbf{x}, \mathbf{y}, \mathbf{y}^p}(\mathbf{x} = \hat{x}, \mathbf{y} = y, \mathbf{y}^p = y^p),$$

where the notations $\mathbf{x} = \hat{x}$, $\mathbf{y} = y$, and $\mathbf{y}^p = y^p$ mean that the random variables \mathbf{x} , \mathbf{y} , and \mathbf{y}^p take some deterministic values \hat{x} , y , and y^p , respectively.

Lemma 1 For system (1), the joint probability density function $f_{\mathbf{x}, \mathbf{y}, \mathbf{y}^p}(\hat{x}, y, y^p)$ at step $k + 1$ is equivalent to

$$\begin{aligned} & f_{\mathbf{x}, \mathbf{y}, \mathbf{y}^p}(\hat{x}, y, y^p) \\ &= \text{constant} \times \exp\left(-\frac{1}{2}(\hat{x}_0 - \bar{x}_0)^T P_0^{-1}(\hat{x}_0 - \bar{x}_0)\right) \\ & \quad \times \prod_{t=0}^k \exp\left(-\frac{1}{2}\hat{\omega}_t^T Q^{-1}\hat{\omega}_t - \frac{1}{2}\hat{\nu}_{t+1}^T R^{-1}\hat{\nu}_{t+1}\right) \\ & \quad \times \prod_{i=1}^N \exp\left(-\frac{1}{2}(\hat{\xi}^i)^T P_\xi^{-1}\hat{\xi}^i\right) \\ & \quad \times \prod_{i=1}^N \prod_{h=0}^{L-1} \exp\left(-\frac{1}{2}(\hat{\omega}_h^i)^T Q^{-1}\hat{\omega}_h^i\right) \\ & \quad \times \prod_{i=1}^N \prod_{h=0}^L \exp\left(-\frac{1}{2}(\hat{\nu}_h^i)^T R^{-1}\hat{\nu}_h^i\right) \\ & \triangleq f(\hat{x}_0, \hat{\omega}, \hat{\nu}, \hat{\xi}^p, \hat{\omega}^p, \hat{\nu}^p), \end{aligned} \tag{12}$$

where \hat{x}_0 , $\hat{\omega}$, and $\hat{\nu}$ are variables defined above (5) with their elements satisfying (5); and

$$\begin{aligned}\hat{\omega}^P &= [(\hat{\omega}^1)^T, \dots, (\hat{\omega}^N)^T]^T, \quad \hat{\omega}^i = [(\hat{\omega}_0^i)^T, \dots, (\hat{\omega}_{L-1}^i)^T]^T, \\ \hat{\nu}^P &= [(\hat{\nu}^1)^T, \dots, (\hat{\nu}^N)^T]^T, \quad \hat{\nu}^i = [(\hat{\nu}_0^i)^T, \dots, (\hat{\nu}_L^i)^T]^T, \\ \hat{\xi}^P &= [(\hat{\xi}^1)^T, \dots, (\hat{\xi}^N)^T]^T,\end{aligned}$$

are variables with their elements satisfying

$$\begin{aligned}y_h^i &= CA^h(\bar{x}_0^i + \hat{\xi}^i) + \sum_{l=1}^h CA^{l-1}(Bu_{h-l}^i + \hat{\omega}_{h-l}^i) + \hat{\nu}_h^i, \\ \forall h &= 1, \dots, L,\end{aligned}\quad (13)$$

$$\text{and } y_0^i = C(\bar{x}_0^i + \hat{\xi}^i) + \hat{\nu}_0^i.$$

The proof of Lemma 1 is given in Appendix 9.1.

As stated in Section 2.1, in the model-based filtering case, the *a posteriori* MMSE state estimate \hat{x}_k , $k \in \mathbb{N}$, defined in (3), corresponds to the optimal solution of variables \hat{x} to the ML-based optimization problem (6). That is, the state estimate of system (1) can be obtained by solving (6). Inspired by this idea, in the data-driven filtering case, we perform state estimation for system (1) by maximizing the likelihood function $f(\hat{x}_0, \hat{\omega}, \hat{\nu}, \hat{\xi}^P, \hat{\omega}^P, \hat{\nu}^P)$, i.e.,

$$\begin{aligned}\underset{\hat{x}_0, \hat{\omega}, \hat{\nu}, \hat{\xi}^P, \hat{\omega}^P, \hat{\nu}^P}{\text{minimize}} \quad & -\ln f(\hat{x}_0, \hat{\omega}, \hat{\nu}, \hat{\xi}^P, \hat{\omega}^P, \hat{\nu}^P) \\ \text{s.t.} \quad & \text{(5) and (13)}.\end{aligned}\quad (14)$$

By solving (14) at step $k+1$, we can obtain the optimal values of variables \hat{x}_t in the constraint (5), denoted by \hat{x}_t^* , $t = 0, \dots, k+1$. Then, we let \hat{x}_t^* , $t = 0, \dots, k+1$, be the estimate of the state x_t , $t = 0, \dots, k+1$, respectively.

To solve (14) with known A , B , and C , some existing algorithms may be applied, e.g., the alternating direction method of multipliers (ADMM) [38]. However, when A , B , and C are unknown and one attempts to solve (14) by removing them in the constraints, there may exist complex coupling terms between two sets of variables $\{\hat{x}_0, \hat{\omega}, \hat{\nu}\}$ and $\{\hat{\xi}^P, \hat{\omega}^P, \hat{\nu}^P\}$. For example, when representing A using $\{y, \hat{\xi}^P, \hat{\omega}^P, \hat{\nu}^P\}$, e.g., $A = f_A(y, \hat{\xi}^P, \hat{\omega}^P, \hat{\nu}^P)$, and substituting this representation into constraint (5), there will create a multiplicative coupling term $f_A(y, \hat{\xi}^P, \hat{\omega}^P, \hat{\nu}^P)\hat{x}_0$. This indicates that when A , B , and C are unknown, the optimization problem (14) becomes nonlinear and non-convex. Hence, the optimal solution $\{\hat{x}_t^*\}_{t=0}^k$ to (14) at step k may be different from the optimal solution $\{\hat{x}_t^*\}_{t=0}^{k+1}$ at step $k+1$. This means that there lacks a recursion between \hat{x}_k^* in $\{\hat{x}_t^*\}_{t=0}^k$ and \hat{x}_{k+1}^* in $\{\hat{x}_t^*\}_{t=0}^{k+1}$. Therefore, even when we have obtained \hat{x}_k^* at step k , we cannot use it to derive \hat{x}_{k+1}^* at step $k+1$.

Algorithm 1 Recursive Data-Driven Kalman Filter.

Input: U, Y, \bar{X}_0, u , and y , defined in (10) and (2);

Output: \hat{x}_k , $k \in \mathbb{N}$;

1: compute the values of matrices $A_\#$, $B_\#$, and $C_\#$:

$$A_\# = G_{1,\#}^\dagger G_{2,\#}, \quad (15a)$$

$$B_\# = G_{1,\#}^\dagger G_{3,\#}, \quad (15b)$$

$$C_\# = G_{4,\#} = G_{1,\#}(1:p; 1:n), \quad (15c)$$

with

$$G_{1,\#} = \left(Y \begin{bmatrix} \bar{X}_0 \\ U \end{bmatrix}^\dagger \right) (1:Lp; 1:n),$$

$$G_{2,\#} = \left(Y \begin{bmatrix} \bar{X}_0 \\ U \end{bmatrix}^\dagger \right) (p+1:Lp+p; 1:n),$$

$$G_{3,\#} = \left(Y \begin{bmatrix} \bar{X}_0 \\ U \end{bmatrix}^\dagger \right) (p+1:Lp+p; n+1:2n);$$

2: **for** $k = 0, 1, \dots$ **do**

$$\hat{x}_{k+1|k} = A_\# \hat{x}_k + B_\# u_k,$$

$$\hat{x}_{k+1} = \hat{x}_{k+1|k} + L_{k+1}^\# (y_{k+1} - C_\# \hat{x}_{k+1|k}),$$

$$L_{k+1}^\# = \bar{P}_{k+1}^\# C_\#^T (R + C_\# \bar{P}_{k+1}^\# C_\#^T)^{-1}, \quad (16)$$

$$\bar{P}_{k+1}^\# = A_\# P_k^\# A_\#^T + Q,$$

$$P_{k+1}^\# = \bar{P}_{k+1}^\# - \bar{P}_{k+1}^\# C_\#^T (R + C_\# \bar{P}_{k+1}^\# C_\#^T)^{-1} C_\# \bar{P}_{k+1}^\#,$$

where \hat{x}_{k+1} is the estimate of the state x_{k+1} in (1), $\hat{x}_0 = \bar{x}_0$, and $P_0^\# = P_0$;

3: **end for**

Subsequently, the problem (14) has to be solved at every step, and the computation complexity (see the dimensions of the optimization variables) increases with respect to k . This issue will be addressed in the next subsection.

3.2 Recursive Data-Driven Kalman Filter

In this subsection, we present a computation-friendly method for solving (14). We use the solution to (14) at time step k to facilitate the solving of this problem at time step $k+1$.

To proceed, we let $\hat{\omega}_{0:k-1}$ and $\hat{\nu}_{1:k}$ denote the optimization variables $\hat{\omega}$ and $\hat{\nu}$ in (14) at time step k , $k \geq 1$, and denote the optimization variables $\hat{\omega}$ and $\hat{\nu}$ at step $k+1$ as $\hat{\omega} = [\hat{\omega}_{0:k-1}^T, \hat{\omega}_k^T]^T$ and $\hat{\nu} = [\hat{\nu}_{1:k}^T, \hat{\nu}_{k+1}^T]^T$. By combining with $\{\hat{x}_0, \hat{\xi}^P, \hat{\omega}^P, \hat{\nu}^P\}$, all variables to be optimized

at step $k + 1$ can be divided into two segments:

$$\{\hat{x}_0, \hat{\omega}_{0:k-1}, \hat{\nu}_{1:k}, \hat{\xi}^P, \hat{\omega}^P, \hat{\nu}^P\} \quad \text{and} \quad \{\hat{\omega}_k, \hat{\nu}_{k+1}\}.$$

Let $\{\hat{x}_0^*, \hat{\omega}^*, \hat{\nu}^*, \hat{\xi}^{P*}, \hat{\omega}^{P*}, \hat{\nu}^{P*}\}_k$ denote the solution to (14) solved at time step k . Then, we let the first segment of variables at time step $k + 1$ equal to the solution obtained at time step k , i.e.,

$$\begin{aligned} & \{\hat{x}_0, \hat{\omega}_{0:k-1}, \hat{\nu}_{1:k}, \hat{\xi}^P, \hat{\omega}^P, \hat{\nu}^P\} \\ = & \{\hat{x}_0^*, \hat{\omega}^*, \hat{\nu}^*, \hat{\xi}^{P*}, \hat{\omega}^{P*}, \hat{\nu}^{P*}\}_k, \quad \forall k \in \mathbb{N}. \end{aligned} \quad (17)$$

The initial solution $\{\hat{x}_0^*, \hat{\omega}^*, \hat{\nu}^*, \hat{\xi}^{P*}, \hat{\omega}^{P*}, \hat{\nu}^{P*}\}_0$ is obtained by solving

$$\begin{aligned} & \underset{\hat{x}_0, \hat{\omega}_{0:-1}, \hat{\nu}_{1:0}, \hat{\xi}^P, \hat{\omega}^P, \hat{\nu}^P}{\text{minimize}} && -\ln f(\hat{x}_0, \hat{\omega}_{0:-1}, \hat{\nu}_{1:0}, \hat{\xi}^P, \hat{\omega}^P, \hat{\nu}^P) \\ & \text{s.t.} && \hat{\omega}_{0:-1} = 0, \hat{\nu}_{1:0} = 0, \text{ and (13)}. \end{aligned}$$

where $\hat{\omega}_{0:-1}$ and $\hat{\nu}_{1:0}$ are set to be zero for self-consistency. By adding the recursive design (17), the problem (14) is converted to the following optimization problem

$$\begin{aligned} & \underset{\hat{x}_0, \hat{\omega}, \hat{\nu}, \hat{\xi}^P, \hat{\omega}^P, \hat{\nu}^P}{\text{minimize}} && -\ln f(\hat{x}_0, \hat{\omega}, \hat{\nu}, \hat{\xi}^P, \hat{\omega}^P, \hat{\nu}^P) \\ & \text{s.t.} && (5), (13), \text{ and (17)}. \end{aligned} \quad (18)$$

In comparison to (14), an extra constraint (17) is added into (18). By doing so, the new optimization problem (18) becomes convex, whose solution can be expressed in a closed form as shown in Appendix 9.2. In addition, only two variables $\hat{\omega}_{k-1}$ and $\hat{\nu}_k$ need to be optimized at each time step k , $\forall k \in \mathbb{N}^+$. Hence, the computation burden is reduced.

By following the argument above (14), we let the optimal solutions of variables \hat{x}_t , $t = 0, \dots, k + 1$, to (18) be the state estimates of system (1). The filtering process can be specified as Algorithm 1, which is called the DDKF. Algorithm 1 corresponds to the framework $g(\cdot)$ defined in Section 2.3. The derivation of Algorithm 1 is provided in Appendix 9.2.

In Algorithm 1, A_{\sharp} , B_{\sharp} , and C_{\sharp} are the estimates of A , B , and C , respectively; $\hat{x}_{k+1|k}$ and \hat{x}_{k+1} are variables to approximate the *a priori* and *a posteriori* state estimates of system (1) at step $k + 1$, respectively; and L_{k+1}^{\sharp} , \bar{P}_{k+1}^{\sharp} , and P_{k+1}^{\sharp} are the recursive filter parameters. In addition, the matrix $G_{1,\sharp}$ in Algorithm 1 is required to have full column rank to guarantee the existence of $G_{1,\sharp}^{\dagger}$. In the next section, we will show this hypothesis always holds with any high probability under Assumptions 1 and 2 by selecting an appropriate N .

It can be seen from Algorithm 1 that the proposed data-driven filter obtained by solving (18) comprises two

processes: system matrices identification (15) and certainty equivalence Kalman filtering (16). This structure coincides with the identification-based filtering framework proposed in the literature. However, the proposed method (15) has two special advantages compared with the traditional identification methods that mainly follow the subspace approach [23] or the prediction error approach [39]. Specifically, the subspace approach usually generates a state-space realization up to a similarity transformation, rather than the original one of physical meaning [40]. The prediction error approach estimates A , B , and C by directly maximizing a non-convex prediction error cost function, while the numerical searches of optimal solutions make it challenging to quantify the estimation performance. In particular, it is hard to find a closed-form relation between the performance and the data informativity. In contrast, the identification method (15) determines a state-space realization exactly matching (1), which is achieved by leveraging both the multiple input-output trajectories and the means of the associated initial states. Moreover, the filtering performance of the proposed DDKF can be explicitly evaluated, as demonstrated in the following sections.

4 Data Informativity Analysis

This section is aimed to analyze the necessary informativity of the pre-collected data required for performing the DDKF (16). The necessary number of the pre-collected system trajectories for ensuring the full column rank of $G_{1,\sharp}$ in Algorithm 1 is analyzed.

According to (11), we define two auxiliary matrices Z and Z_{\sharp} as

$$Z \triangleq [G \quad H(I_L \otimes B)], \quad (19)$$

$$Z_{\sharp} \triangleq [G_{\sharp} \quad H_{\sharp}(I_L \otimes B_{\sharp})], \quad (20)$$

where G_{\sharp} , H_{\sharp} , and B_{\sharp} denote the estimates of G , H , and B obtained by solving (18), respectively. Let $e_Z = Z_{\sharp} - Z$ be the error between Z and Z_{\sharp} . It follows from (11) that

$$\begin{aligned} e_Z &= Y \begin{bmatrix} \bar{X}_0 \\ U \end{bmatrix}^{\dagger} - (Y - G\Xi - H\Omega - V) \begin{bmatrix} \bar{X}_0 \\ U \end{bmatrix}^{\dagger} \\ &= (G\Xi + H\Omega + V) \begin{bmatrix} \bar{X}_0 \\ U \end{bmatrix}^T \left(\begin{bmatrix} \bar{X}_0 \\ U \end{bmatrix} \begin{bmatrix} \bar{X}_0 \\ U \end{bmatrix}^T \right)^{-1}, \end{aligned} \quad (21)$$

where the second equality is obtained by substituting the explicit expression of $([\bar{X}_0^T, U^T]^T)^{\dagger}$. Besides, in the experiments of generating data, let $u_h^i \sim \mathcal{N}(0, S)$ and $\bar{x}_0^i \sim \mathcal{N}(0, P_{\bar{x}_0})$ with $S \in \mathbb{R}^{m \times m} > 0$ and $P_{\bar{x}_0} \in \mathbb{R}^{n \times n} > 0$ be mutually uncorrelated, $\forall h \in \{0, 1, \dots, L-1\}$, $\forall i \in \mathcal{V}$. We let covariances $Q = \sigma_{\omega}^2 I_n$, $R = \sigma_{\nu}^2 I_p$, $S = \sigma_u^2 I_m$, $P_{\xi} = \sigma_{\xi}^2 I_n$, and $P_{\bar{x}_0} = \sigma_{\bar{x}_0}^2 I_n$ for notational simplicity.

Note that the results obtained in this section still hold without this simplification but will be in a more complicated form. Now, we have an important result about e_Z .

Proposition 1 Consider system (1) with the collected data U , Y , and \bar{X}_0 defined in (10). Suppose Assumption 3 holds. If $N \geq 8(n + Lm) + 2(Lp + Lm + Ln + p + n + 3)\log(4/\delta)$, then the following inequality holds with probability at least $1 - \delta$

$$\|e_Z\|_2 \leq \mathcal{O}\left(\sqrt{\frac{\log(36/\delta)}{N}}\right), \quad (22)$$

where $\delta \in (0, 1)$ is any small positive scalar.

The proof of Proposition 1 is provided in Appendix 9.3.

Let G_1 , G_2 , and G_3 represent the corresponding block matrices in Z as $G_{1,\#}$, $G_{2,\#}$, and $G_{3,\#}$ in $Z_\#$, respectively, where $G_{1,\#}$, $G_{2,\#}$, and $G_{3,\#}$ are defined below (15). According to Proposition 1, we can directly have the following corollary using the union bound.

Corollary 1 Consider system (1) with the pre-collected data U , Y , and \bar{X}_0 , defined in (10). Suppose Assumption 3 holds. For any positive scalars $\epsilon_G \in (0, 1)$ and $\delta \in (0, 1)$, there always exists a positive integer $N_G(\epsilon_G, \delta)$ such that when $N \geq N_G(\epsilon_G, \delta)$,

$$\begin{aligned} \|G_1 - G_{1,\#}\|_2 &\leq \epsilon_G, \\ \|G_2 - G_{2,\#}\|_2 &\leq \epsilon_G, \\ \|G_3 - G_{3,\#}\|_2 &\leq \epsilon_G, \end{aligned}$$

hold with probability at least $1 - \delta$.

From the proof of Proposition 1, one feasible $N_G(\epsilon_G, \delta)$ is given by

$$N_G(\epsilon_G, \delta) = \left\lceil \max \left\{ 8(n + Lm) + 2(Lp + Lm + Ln + p + n + 3)\log(12/\delta), \frac{L\log(108/\delta)M_Z^2}{\epsilon_G^2} \right\} \right\rceil, \quad (23)$$

where $\lceil \cdot \rceil$ is the function of rounding up to the nearest integer, and M_Z is a positive constant defined as

$$M_Z = 16\sqrt{L}\sigma_{\max}\sigma_{\min}^{-2} \left[\rho(G)\sigma_\xi\sqrt{2+m} + \rho(H)\sigma_\omega\sqrt{1+n+m} + \sigma_\nu\sqrt{1+2p+m} \right], \quad (24)$$

with $\sigma_{\max} = \max\{\sigma_{\bar{x}_0}, \sigma_u\}$ and $\sigma_{\min} = \min\{\sigma_{\bar{x}_0}, \sigma_u\}$.

It can be found from (23) and (24) that the estimation accuracy of the matrices G_1 , G_2 , and G_3 is dependent on the parameters σ_ξ , σ_ω , and σ_ν , which represent the characteristics of the noise terms ξ^i , $\omega_h^{i,p}$ and $\nu_h^{i,p}$ in the

pre-collected data. Specifically, if these noise terms have larger covariances, leading to an increased M_Z , a correspondingly larger number of previous trajectories are required to maintain a given accuracy. On the other hand, if there exists no system noise, we have $N_G(\epsilon_G, \delta) = 0$. In this case, the condition in Assumption 3 is sufficient to ensure accurate estimation of G_1 , G_2 , and G_3 .

Based on Corollary 1, we determine the necessary number of the pre-collected trajectories required for ensuring the full column rank of $G_{1,\#}$, i.e., the necessary number required for performing the proposed DDKF.

Proposition 2 Suppose Assumptions 1, 2 and 3 hold. If $N \geq N_G(\epsilon_G, \delta)$ and $\epsilon_G < \epsilon_0$, where $N_G(\epsilon_G, \delta)$ is defined in (23) and ϵ_0 is defined as

$$\epsilon_0 \triangleq \sqrt{\|G_1\|_2^2 + \lambda_{\min}(G_1^T G_1)} - \|G_1\|_2, \quad (25)$$

then $G_{1,\#}$ has full column rank with probability at least $1 - \delta$.

The proof of Proposition 2 is provided in Appendix 9.4. From this proof, ϵ_0 can also be chosen as

$$\epsilon_0 \triangleq \sqrt{\|G_{1,\#}\|_2^2 + \lambda_{\min}(G_{1,\#}^T G_{1,\#})} - \|G_{1,\#}\|_2,$$

which depends on the pre-collected data. Proposition 2 reveals that $G_{1,\#}$ always has full column rank with any high probability if the number of the pre-collected system trajectories is large enough.

5 DDKF Performance Evaluation

In this section, a sample-complexity bound for evaluating the estimation accuracy of matrices A , B , and C is derived as a preliminary. Then, the estimation performance of the DDKF (16) is evaluated from two aspects: 1) the uniform boundedness and convergence of the DDKF parameters; 2) the performance gap between the DDKF and the traditional Kalman filter with accurate system matrices.

5.1 Accuracy Analysis of Optimized System Matrices

In this subsection, the estimation accuracy of matrices A , B , and C is analyzed.

Proposition 3 Suppose Assumptions 1, 2 and 3 hold. For any positive scalars $\epsilon < \epsilon_0$ and $\delta \in (0, 1)$, there always exists a positive integer $N_0(\epsilon, \delta)$ such that if $N \geq N_0(\epsilon, \delta)$, then

$$\|A - A_\# \|_2 \leq \epsilon, \|B - B_\# \|_2 \leq \epsilon, \|C - C_\# \|_2 \leq \epsilon,$$

hold with probability at least $1 - \delta$. Particularly, one feasible $N_0(\epsilon, \delta)$ is given by

$$N_0(\epsilon, \delta) = \left\lceil \max \left\{ 8(n + Lm) + 2(Lp + Lm + Ln + p + n + 3)\log(36/\delta), \frac{L\log(324/\delta)M^2}{\epsilon^2} \right\} \right\rceil, \quad (26)$$

where $M = \max\{M_A, M_B, M_C\}$ with

$$M_A = \frac{(\|A\|_2 + 1)M_Z}{\sqrt{\lambda_{\min}(G_1^T G_1) - \epsilon^2 - 2\epsilon\|G_1\|_2}},$$

$$M_B = \frac{(\|B\|_2 + 1)M_Z}{\sqrt{\lambda_{\min}(G_1^T G_1) - \epsilon^2 - 2\epsilon\|G_1\|_2}},$$

$$M_C = M_Z, \text{ defined in (24).}$$

The proof of Proposition 3 is provided in Appendix 9.5.

Similar to the results in [18, 19], $N_0(\epsilon, \delta)$ in Proposition 3 depends on the upper bounds of system matrices. However, different from these works where the system matrices are identified in a coupled manner [19], or the state-input data are needed [18], in this paper, every system matrix constituting the exact realization (1) can be estimated separately only using the input-output data together with the means of the initial states. Moreover, the results obtained in Proposition 3 can, in turn, be used to check whether Assumption 1 holds. Specifically, it can be checked by replacing A and C by $A_{\#}$ and $C_{\#}$, respectively, when the number of samples is sufficiently large.

5.2 Properties of Recursive Parameters $\bar{P}_{k+1}^{\#}$ and $P_{k+1}^{\#}$

In this subsection, the uniform boundedness and convergence of the DDKF parameters defined in (16) are ensured. Since the performance analysis with $B_{\#}$ and $C_{\#}$ is the same as the one with $A_{\#}$, we assume $B_{\#} = B$ and $C_{\#} = C$ for notational simplicity. According to Proposition 2 and Proposition 3, $G_{1,\#}$ has full column rank with probability at least $1 - \delta$ when $N \geq N_0(\epsilon, \delta)$ and $\epsilon < \epsilon_0$. That is, $(C, A_{\#})$ is observable [37, Theorem 6.DO1]. Hence, similarly to the parameter iteration in Kalman filtering, $\bar{P}_{k+1}^{\#}$ and $P_{k+1}^{\#}$ in (16) exponentially converge to the unique solution to

$$\begin{aligned} \bar{P}_{\#} &= A_{\#} P_{\#} A_{\#}^T + Q, \\ P_{\#} &= \bar{P}_{\#} - \bar{P}_{\#} C^T (R + C \bar{P}_{\#} C^T)^{-1} C \bar{P}_{\#}, \end{aligned} \quad (27)$$

with probability at least $1 - \delta$ when $N \geq N_0(\epsilon, \delta)$ and $\epsilon < \epsilon_0$. This also indicates that $\bar{P}_{k+1}^{\#}$ and $P_{k+1}^{\#}$ are uniformly bounded.

In addition, \bar{P}_{k+1} defined in (4) converges to \bar{P} exponentially, where

$$\begin{aligned} \bar{P} &= A P A^T + Q, \\ P &= \bar{P} - \bar{P} C^T (R + C \bar{P} C^T)^{-1} C \bar{P}. \end{aligned} \quad (28)$$

In the following, the error between $\bar{P}_{k+1}^{\#}$ and \bar{P} and the error between $P_{k+1}^{\#}$ and P are quantified.

Proposition 4 *Suppose Assumptions 1, 2 and 3 hold. If $N \geq N_0(\epsilon, \delta)$ and $\epsilon < \epsilon_0$ with $N_0(\epsilon, \delta)$ and ϵ_0 being defined in (26) and (25), respectively, then*

$$\|\bar{P}_{\#} - \bar{P}\|_2 \leq \mathcal{O}\left(\sqrt{\frac{\log(1/\delta)}{N}}\right),$$

or

$$\|P_{\#} - P\|_2 \leq \mathcal{O}\left(\sqrt{\frac{\log(1/\delta)}{N}}\right),$$

holds with probability at least $1 - \delta$.

The proof of Proposition 4 is provided in Appendix 9.6. Proposition 4 will contribute to the performance evaluation of the proposed DDKF in the next subsection.

5.3 Performance Evaluation of DDKF

In this part, the estimation performance gap between the designed DDKF (16) and the traditional Kalman filter (4) is derived. Since the filter parameters in (16) converge exponentially, as discussed in Section 5.2, we assume they are in their steady states for notational simplicity. Specifically, let $L_{k+1}^{\#} = L^{\#} \triangleq \bar{P}^{\#} C^T (R + C \bar{P}^{\#} C^T)^{-1}$, where $\bar{P}^{\#}$ is defined in (27). In addition, the following assumption on the state x_k is needed.

Assumption 4 *The covariance of x_k is uniformly upper bounded, i.e., there exists a positive definite matrix Π such that $\mathbb{E}\{x_k x_k^T\} \leq \Pi, \forall k \in \mathcal{N}$.*

Assumption 4 holds for many physical systems with closed-loop controllers. In particular, two types of data-driven controllers will be designed for system (1) to guarantee this assumption in Section 6.

Now, we define $e_k = \hat{x}_k - x_k$ as the state estimation error of the designed DDKF (16) at step k , and $P_{e,k} \triangleq \mathbb{E}\{e_k e_k^T\}$ as the associated covariance. One significant result about the estimation performance of the proposed DDKF is given as follows.

Theorem 1 *Consider system (1) with the pre-collected data U, Y , and \bar{X}_0 defined in (10). Suppose Assumptions*

1, 2, 3 and 4 hold. When $N \geq N_0(\epsilon, \delta)$ and $\epsilon < \epsilon_0$ with $N_0(\epsilon, \delta)$ and ϵ_0 being defined in (26) and (25), respectively, then

$$\|P_{e,\infty} - P\|_2 \leq \mathcal{O}\left(\sqrt{\frac{\log(1/\delta)}{N}}\right),$$

holds with probability at least $1 - 2\delta$.

The proof of Theorem 1 is provided in Appendix 9.7.

From Theorem 1, we have $\|P_{e,\infty} - P\|_2 \rightarrow 0$ when $N \rightarrow \infty$. In this case, the performance of the designed DDKF is as good as the Kalman filter with known system matrices. Recent works [23, 24] introduced a ‘‘system identification + Kalman filtering’’ method for data-driven filtering of system (1). It can guarantee a performance like

$$\|\hat{P}_{e,\infty} - U_T P U_T^{-1}\|_2 \leq \mathcal{O}\left(\sqrt{\frac{\log(1/\delta)}{N}}\right),$$

where $\hat{P}_{e,k} \triangleq \mathbb{E}\{(\hat{x}_k - U_T x_k)(\hat{x}_k - U_T x_k)^T\}$ and U_T is an unknown invertible matrix. The system state estimated by this method corresponds to a balanced state-space realization up to an unknown similarity transformation, rather than the original one (1). Meanwhile, it requires A to be marginally stable. On the contrary, the proposed DDKF (16) determines the exact realization (1) and allows A to be unstable, but requires some knowledge of the initial state.

6 Data-Driven Output Feedback Control

In this section, the state estimates of the DDKF (16) are used for data-driven feedback control. First, a static data-driven output feedback controller is designed to stabilize system (1). Then, a dynamic one (LQG control) is proposed.

6.1 Static Output Feedback Control

A static output feedback controller is designed for system (1) as

$$u_k = K_s y_k, \quad (29)$$

where $K_s \in \mathbb{R}^{m \times p}$ is the controller gain to be designed. Substituting the above controller into (1) yields

$$\begin{aligned} x_{k+1} &= A x_k + B K_s y_k + \omega_k \\ &= (A + B K_s C) x_k + B K_s \nu_k + \omega_k. \end{aligned} \quad (30)$$

To ensure the stability of the closed-loop system (30), it suffices to render $A + B K_s C$ Schur stable by designing the controller gain K_s using the pre-collected data U, Y , and \bar{X}_0 defined in (10).

Assumption 5 (A, B) is controllable.

Now, the stability analysis of the static output feedback controller (29) is given below.

Theorem 2 Suppose Assumptions 1, 2, 3 and 5 hold, and there exists a matrix $Q_K = [Q_1^T, Q_2^T]^T \in \mathbb{R}^{(m+n) \times n}$ and a positive definite matrix $\Delta \in \mathbb{R}^{n \times n}$ such that

$$\begin{bmatrix} Q_1 - \Delta & * \\ *^T & Q_1 \end{bmatrix} > 0, \quad Q_1 > 0, \quad (31)$$

where $* = G_{1,\#}^\dagger (G_{2,\#} Q_1 + G_{3,\#} Q_2)$ with $G_{1,\#}, G_{2,\#}$ and $G_{3,\#}$ being defined in Algorithm 1. If $N \geq N_0(\epsilon, \delta)$ and $\epsilon < \min\{\epsilon_0, \epsilon_1\}$ with $N_0(\epsilon, \delta), \epsilon_0$ and ϵ_1 defined in (26), (25) and (41), respectively, then the output feedback control input u_k designed in (29) with any K_s satisfying

$$K_s G_{4,\#} Q_1 = Q_2,$$

stabilizes system (1) with probability at least $1 - \delta$, where $G_{4,\#}$ is defined in Algorithm 1.

The proof of Theorem 2 is provided in Appendix 9.8.

The linear matrix inequalities (LMIs) in (31) are fully constructed by the pre-collected system data. Further, Theorem 2 gives rise to two more precise corollaries.

Corollary 2 Suppose all conditions in Theorem 2 hold and $G_{4,\#}$ has full row rank. Then, K_s in (29) can be designed in closed-form

$$K_s = Q_2 G_{4,\#}^T (G_{4,\#} Q_1 G_{4,\#}^T)^{-1}.$$

Corollary 3 Suppose all conditions in Theorem 2 hold. Then, the expectation of the squared state is uniformly bounded, i.e., Assumption 4 holds.

In the proposed static data-driven controller (29), K_s should satisfy $K_s G_{4,\#} Q_1 = Q_2$, which may have no feasible solution. To bypass this constraint, a dynamic data-driven output feedback controller will be proposed in the following part.

6.2 Dynamic Output Feedback Control

A dynamic output feedback controller is designed for system (1) as

$$u_k = K_d \hat{x}_k, \quad (32)$$

where \hat{x}_k is the state estimate obtained from the DDKF (16), and $K_d \in \mathbb{R}^{m \times n}$ is the controller gain, which is designed as follows.

Theorem 3 Suppose Assumptions 1, 2, 3 and 5 hold, and there exists a matrix $Q_K = [Q_1^T, Q_2^T]^T$ and a positive definite matrix Δ satisfying (31). Then, the dynamic output feedback controller (32) with

$$K_d = Q_2 Q_1^{-1},$$

stabilizes system (1) with probability at least $1 - \delta$, if $N \geq N_0(\epsilon, \delta)$ and $\epsilon < \min\{\epsilon_0, \epsilon_1, \epsilon_2\}$, where $N_0(\epsilon, \delta)$, ϵ_0 , ϵ_1 and ϵ_2 are defined in (26), (25), (41) and (42), respectively.

The proof of Theorem 3 is given in Appendix 9.9.

Further, we consider an LQG control problem for system (1), where the cost function is defined as

$$J_{\text{LQG}} = \mathbb{E} \left\{ \sum_{h=0}^{\infty} (x_h^T S_1 x_h + u_h^T S_2 u_h) \right\}, \quad (33)$$

where $S_1 \in \mathbb{R}^{n \times n}$ and $S_2 \in \mathbb{R}^{m \times m}$ are two positive definite matrices. The objective is to minimize the above cost function by designing an optimal control input. In the following, a novel data-driven LQG controller is designed with performance guarantees.

Corollary 4 Suppose Assumptions 1, 2, 3 and 5 hold. There exists a positive integer $N_1(\epsilon, \delta)$ such that when $N \geq N_1(\epsilon, \delta)$, the input u_k designed in (32) with

$$K_d = [(G_{1,\#}^\dagger G_{3,\#})^T P_u G_{1,\#}^\dagger G_{3,\#} + S_2] (G_{1,\#}^\dagger G_{3,\#})^T G_{1,\#}^\dagger G_{2,\#},$$

guarantees

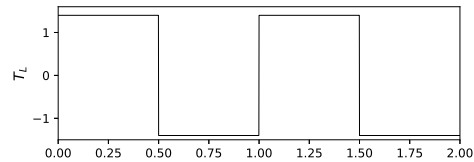
$$\|J_{\text{LQG}} - J^*\|_2 \leq \mathcal{O} \left(\sqrt{\frac{\log(1/\delta)}{N}} \right), \quad (34)$$

with probability at least $1 - \delta$, where

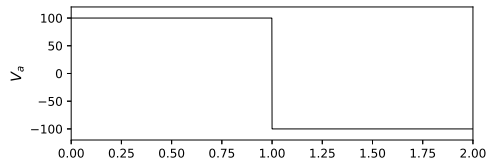
$$P_u = (G_{1,\#}^\dagger G_{2,\#})^T [P_u^{-1} + G_{1,\#}^\dagger G_{3,\#} S_2^{-1} (G_{1,\#}^\dagger G_{3,\#})^T]^{-1} \times G_{1,\#}^\dagger G_{2,\#} + S_1,$$

J^* represents the optimal cost using the model-based LQG controller, and $G_{1,\#}$, $G_{2,\#}$ and $G_{3,\#}$ are defined in Algorithm 1.

Corollary 4 can be proved by combining the results in Theorems 1 and 3. It provides an end-to-end sample-complexity upper bound for the performance gap between the proposed data-driven LQG controller and the model-based LQG controller. Particularly, when N tends to infinity, the controller (32) with K_d designed in Corollary 4 ensures the equivalent performance as the model-based LQG controller. Note that some existing works used system identification together with



(a) The load torque input.



(b) The DC voltage input.

Fig. 1. The input of the motor system.

robust control to address the model-free LQG control problem (33). For instance, Dean et al. [18] proposed a strategy that required full state observations and they were able to guarantee an end-to-end performance like (34). Zheng et al. [20] generalized this result to cases using only input-output data, where the controller gain was designed by numerically solving a quasi-convex optimization problem. By comparison, the controller in Corollary 4 does not require full state observations and can be computed in closed form, which serves as an alternative for model-free LQG control.

7 Simulation

In this section, the effectiveness of the proposed DDKF (16) and the data-driven controller (32) based on the DDKF is illustrated by a numerical simulation of a DC motor system, whose dynamics is described in Example 1 given in Section 1.2.

First, let $x \triangleq [\dot{\theta}, i]^T$, $u \triangleq [T_L, V_a]^T$ and $y \triangleq i$. According to [33, Section 5], the discrete-time model of the DC motor system with sampling time period 0.001s can be described by (1), where

$$A = \begin{bmatrix} 0.9951 & 0.2289 \\ -0.0177 & 0.8672 \end{bmatrix}, \quad B = \begin{bmatrix} -0.4158 & 0.0038 \\ -0.0038 & 0.0301 \end{bmatrix},$$

and $C = [0 \ 1]$. Here, we assume that matrices A and B are unknown. Besides, similarly to [33], let the noise covariances be given as $Q = [[0.20, 0.04]^T, [0.04, 0.04]^T]^T$, $R = 0.03$, $P_\xi = I_2$, and let the control input u be chosen as in Fig. 1.

7.1 Simulation of the Proposed DDKF

A set of data denoted by (7) are collected from numerical experiments with $N = 1000$, $L = 20$ and $\sigma_{\bar{x}_0} = \sigma_u = 10^2$

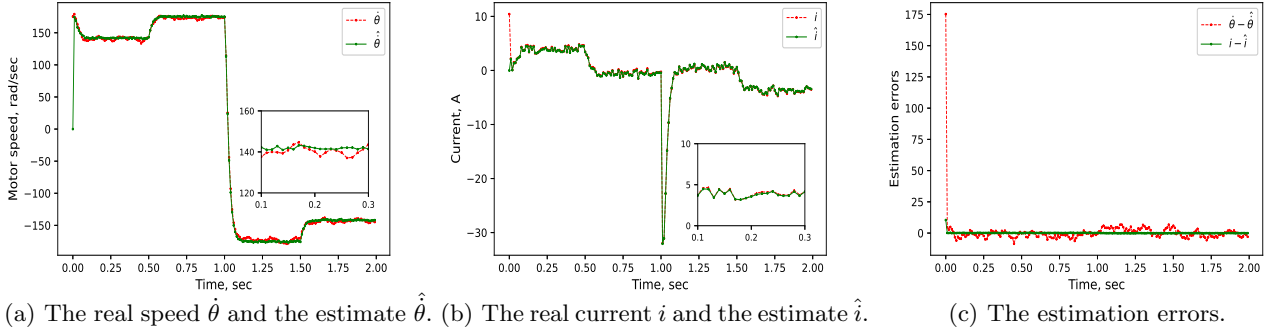


Fig. 2. The comparison between the real motor states and the estimated states using the DDKF (16).

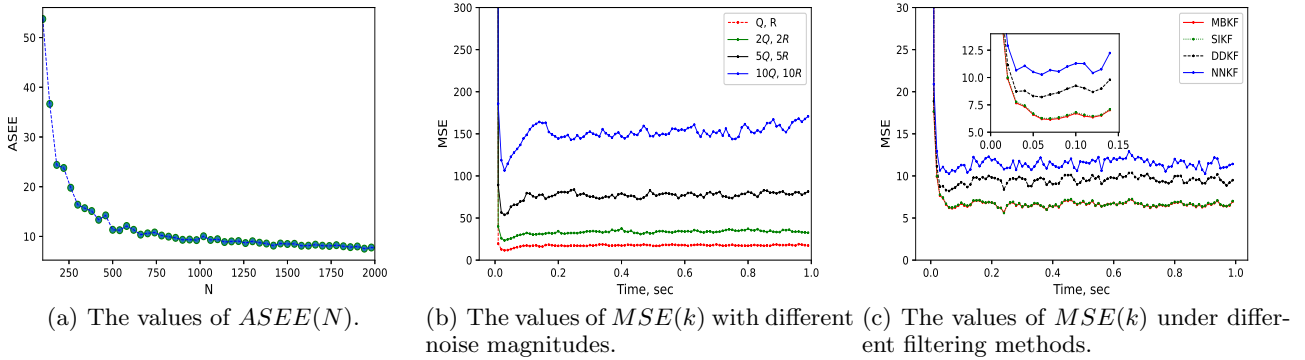


Fig. 3. The influence of several important factors to the estimation performance of the DDKF (16), and the comparison of four filtering methods. Specifically, Fig. (a) illustrates the overall estimation performance of the designed DDKF (16) with respect to the numbers of previous trajectories. Fig. (b) shows the estimation performance of the designed DDKF (16) with different system process and measurement noise magnitudes, where $Q = [[0.20, 0.04]^T, [0.04, 0.04]^T]^T$ and $R = 0.03$. Fig. (c) compares the performance of four filtering methods.

defined below (21). In this part, the aim is to estimate the value of motor speed $\dot{\theta}$ and current i as accurate as possible. To proceed, a mean squared error (MSE) is defined as

$$MSE(k) = \frac{1}{N_t} \sum_{h=1}^{N_t} (\dot{\theta}_k^h - \hat{\dot{\theta}}_k^h)^2,$$

where $\hat{\dot{\theta}}_k^h$ is the estimate of $\dot{\theta}$ at time step k on the h -th trial and $N_t = 2000$ is the number of trials. Besides, an average squared estimation error (ASEE) is defined as

$$ASEE(N) = \frac{1}{N_t \times 1900} \sum_{h=1}^{N_t} \sum_{k=101}^{2000} (\dot{\theta}_k^h - \hat{\dot{\theta}}_k^h)^2,$$

where N denotes the number of the pre-collected trajectories, which is utilized to illustrate the relationship between the estimation performance and the sample complexity.

The real motor states and estimates by the designed DDKF (16) are shown in Fig. 2, where the estimated speed and current well match the actual ones. We also study the influence of two essential factors on the estimation performance of the DDKF (16). Fig. 3-(a) illustrates that the estimation performance of the proposed DDKF is improved with an increasing number of samples, which coincides with the argument in Theorem 1. Fig. 3-(b) shows the relationship between the performance and the noise magnitudes, which is theoretically revealed by the parameter M used in (26).

In addition, three relevant filtering methods in the literature are included for comparison, namely model-based Kalman filter (MBKF) [5], Kalman filter built on system identification (SIKF) [6], and Kalman filter based on neural networks (NNKF) [10, 25]. Note that the MBKF requires accurate system parameters, and the SIKF and NNKF need to collect full state data of previous trajectories, whereas the proposed DDKF relies only on noisy partial states (i.e., measurements). The results depicted in Fig. 3-(c) indicate that the proposed DDKF can guar-

antee a comparable performance to the MBKF, SIKF, and NNKF, but with a much milder requirement on the model information.

7.2 Simulation of the Proposed Controller

Part 2: In this part, the data-driven LQG controller proposed in Corollary 4 is utilized to stabilize the DC motor system. The parameters in (33) are chosen as $S_1 = I_2$, $S_2 = I_2$ and $x_0 = [100, 10]^T$. The input signal for the motor system usually has a form of $u = K\hat{x} + Vu_s$, where u_s denotes a reference trajectory [34]. Without loss of generality, let $u_s = 0$ and the non-zero cases can be directly reformulated into this case when designing the controller [41]. The control performance of the proposed data-driven LQG controller (DDLQG) is compared with the model-based LQG controller (MBLQG) and the system identification-based LQG (SILQG, with full state observations) [18]. For comparison, we define an average cost function as

$$J_{\text{ave}} = \frac{1}{N_t} \sum_{i=1}^{N_t} J_{\text{LQG}}^i,$$

where $N_t = 1000$ is the number of trials, and J_{LQG}^i is the value of J_{LQG} defined in (33) with $0 \leq h \leq 50$ and $N = 500$ in the i -th trail. The values of J_{ave} by utilizing different methods are presented in Table 1, which indicates that the designed DDLQG has the same control performance as the other two methods while eliminating the need for an accurate model and state information.

Table 1
The values of J_{ave} .

	MBLQG	SILQG	DDLQG
J_{ave}	5.158×10^4	5.162×10^4	5.162×10^4

Altogether, these simulation results illustrate the effectiveness of the theoretical results obtained in the paper.

8 Conclusion

This paper has developed a novel DDKF for unknown linear Gaussian systems. Specifically, an ML-based optimization problem has been formulated and solved to construct the state estimates. A sample-complexity upper bound has been derived for the performance gap between the designed DDKF and the Kalman filter with accurate system parameters. Subsequently, two types of data-driven output feedback controllers have been designed to facilitate the implementation of the proposed DDKF. Simulations using a DC motor have demonstrated the effectiveness of the theoretical results. However, many relevant topics deserve in-depth investigation in the future. For example, how to learn state estimators from data for unknown systems affected by non-Gaussian noise remains open, and how to combine prior

information with data for filtering when part of system knowledge is available is also a significant and challenging issue. Our future research will concentrate on these important topics.

9 Appendix

9.1 Proof of Lemma 1

To proceed, similarly to the expression of $f_{\mathbf{x}, \mathbf{y}, \mathbf{y}^P}(\hat{x}, y, y^P)$, the probability density functions of other variables are also simplified, e.g., $f_{\mathbf{y}^P}(\mathbf{y}^P = y^P) = f_{\mathbf{y}^P}(y^P)$. According to the independence of \hat{x} and y from the pre-collected data u^P and y^P , we have

$$f_{\mathbf{x}, \mathbf{y}, \mathbf{y}^P}(\hat{x}, y, y^P) = f_{\mathbf{x}, \mathbf{y}}(\hat{x}, y | u^P, y^P) f_{\mathbf{y}^P}(y^P | u^P), \quad (35)$$

where $f_{\mathbf{x}, \mathbf{y}}(\hat{x}, y | u^P, y^P)$ is the conditional probability density function, denoting the probability density of $\mathbf{x} = \hat{x}$ and $\mathbf{y} = y$ given $\mathbf{u}^P = u^P$ and $\mathbf{y}^P = y^P$. In the following, the closed-form expressions of $f_{\mathbf{x}, \mathbf{y}}(\hat{x}, y | u^P, y^P)$ and $f_{\mathbf{y}^P}(y^P | u^P)$ are deduced.

For $f_{\mathbf{x}, \mathbf{y}}(\hat{x}, y | u^P, y^P)$ at step $k+1$, by utilizing Bayes' rule and the Markovian structure in (1), it can be derived that

$$\begin{aligned} & f_{\mathbf{x}, \mathbf{y}}(\hat{x}, y | u^P, y^P) \\ &= f_{\mathbf{x}_0}(\hat{x}_0) \prod_{t=0}^k f_{\mathbf{x}_{t+1}, \mathbf{y}_{t+1}}(\hat{x}_{t+1}, y_{t+1} | \hat{x}_t, u, u^P, y^P), \end{aligned}$$

where \hat{x}_{t+1} and y_{t+1} are any vectors satisfying (5). Substituting (5) into the above equation yields

$$f_{\mathbf{x}, \mathbf{y}}(\hat{x}, y | u^P, y^P) = f_{\mathbf{x}_0}(\hat{x}_0) \prod_{t=0}^k f_{\omega_t}(\hat{\omega}_t) f_{\nu_{t+1}}(\hat{\nu}_{t+1}), \quad (36)$$

where $\hat{\omega}_t$ and $\hat{\nu}_{t+1}$ are vectors defined in (5). Moreover, according to the definitions of the initial state and system noise in Section 2.1, their probability density functions can be explicitly expressed by

$$f_{\mathbf{s}}(s) = \frac{1}{2\pi^{\dim/2} |\Sigma|^{1/2}} \exp\left(-\frac{1}{2}(s - \mu)^T \Sigma^{-1}(s - \mu)\right),$$

where s represents elements in $\{\hat{x}_0, \hat{\omega}_t, \hat{\nu}_{t+1}\}$ with μ and Σ corresponding to $\{\bar{x}_0, 0, 0\}$ and $\{P_0, Q, R\}$, respectively; and 'dim' denotes the dimension of s . Hence, it

follows from (36) and the above equation that

$$\begin{aligned} & f_{\mathbf{x},\mathbf{y}}(\hat{x}, y|u^{\mathbf{P}}, y^{\mathbf{P}}) \\ &= \text{constant} \times \exp\left(-\frac{1}{2}(\hat{x}_0 - \bar{x}_0)^T P_0^{-1}(\hat{x}_0 - \bar{x}_0)\right) \\ & \times \prod_{t=0}^k \exp\left(-\frac{1}{2}\hat{\omega}_t^T Q^{-1}\hat{\omega}_t - \frac{1}{2}\hat{\nu}_{t+1}^T R^{-1}\hat{\nu}_{t+1}\right). \end{aligned} \quad (37)$$

For the second term $f_{\mathbf{y}^{\mathbf{P}}}(y^{\mathbf{P}}|u^{\mathbf{P}})$ in (35), we can derive from (7) that

$$f_{\mathbf{y}^{\mathbf{P}}}(y^{\mathbf{P}}|u^{\mathbf{P}}) = \prod_{i=1}^N f_{\mathbf{y}^{i,\mathbf{P}}}(y^{i,\mathbf{P}}|u^{i,\mathbf{P}}).$$

Further, according to (9), we have

$$f_{\mathbf{y}^{i,\mathbf{P}}}(y^{i,\mathbf{P}}|u^{i,\mathbf{P}}) = f_{\xi^i}(\hat{\xi}^i) \prod_{h=0}^{L-1} f_{\omega_h^i}(\hat{\omega}_h^i) \prod_{h=0}^L f_{\nu_h^i}(\hat{\nu}_h^i),$$

where $\hat{\xi}^i$, $\hat{\omega}_h^i$, and $\hat{\nu}_h^i$ satisfy (13). Similarly to the derivation process in (37), the expression of $f_{\mathbf{y}^{\mathbf{P}}}(y^{\mathbf{P}}|u^{\mathbf{P}})$ can be computed as

$$\begin{aligned} f_{\mathbf{y}^{\mathbf{P}}}(y^{\mathbf{P}}|u^{\mathbf{P}}) &= \text{constant} \times \prod_{i=1}^N \exp\left(-\frac{1}{2}(\hat{\xi}^i)^T P_{\xi}^{-1}\hat{\xi}^i\right) \\ & \times \prod_{i=1}^N \prod_{h=0}^{L-1} \exp\left(-\frac{1}{2}(\hat{\omega}_h^i)^T Q^{-1}\hat{\omega}_h^i\right) \\ & \times \prod_{i=1}^N \prod_{h=0}^L \exp\left(-\frac{1}{2}(\hat{\nu}_h^i)^T R^{-1}\hat{\nu}_h^i\right). \end{aligned}$$

Now, combining (37) with the above equation gives rise to (12).

9.2 Deduction of Algorithm 1

It suffices to solve the optimization problem (18). First, the optimal \hat{x}_0^* , $\hat{\xi}^{\mathbf{P}*}$, $\hat{\omega}^{\mathbf{P}*}$ and $\hat{\nu}^{\mathbf{P}*}$ at time step 0 can be directly derived as $\hat{x}_0^* = \bar{x}_0$, $\hat{\xi}^{\mathbf{P}*} = 0$, $\hat{\omega}^{\mathbf{P}*} = 0$ and $\hat{\nu}^{\mathbf{P}*} = 0$. Substituting it into (13) gives rise to

$$Y = G_{\#}\bar{X}_0 + H_{\#}(I_L \otimes B_{\#})U = [G_{\#} \ H_{\#}(I_L \otimes B_{\#})] \begin{bmatrix} \bar{X}_0 \\ U \end{bmatrix}.$$

where $G_{\#}$, $H_{\#}$, $A_{\#}$, $B_{\#}$, and $C_{\#}$ denote the estimates of G , H , A , B , and C , respectively. When Assumption 3 holds, there exists a right inverse $([\bar{X}_0^T, U^T]^T)^{\dagger}$ of $[\bar{X}_0^T, U^T]^T$ that $[\bar{X}_0^T, U^T]^T ([\bar{X}_0^T, U^T]^T)^{\dagger} = I_{n+Lm}$. By

post-multiplying both sides of the above equation by $([\bar{X}_0^T, U^T]^T)^{\dagger}$, we have

$$[G_{\#} \ H_{\#}(I_L \otimes B_{\#})] = Y \begin{bmatrix} \bar{X}_0 \\ U \end{bmatrix}^{\dagger}.$$

According to the definitions of $G_{1,\#}$, $G_{2,\#}$, and $G_{3,\#}$ below (15) and the associated structures with respect to $A_{\#}$, $B_{\#}$ and $C_{\#}$, the following equations always hold

$$\begin{aligned} G_{1,\#}A_{\#} &= G_{2,\#}, \\ G_{1,\#}B_{\#} &= G_{3,\#}, \\ C_{\#} &= G_{1,\#}(1 : m; 1 : n). \end{aligned}$$

Further, if $G_{1,\#}$ has full column rank, we can directly obtain (15). Now, the problem (18) becomes a standard quadratic programming problem, which is the same as the traditional optimization problem formulated in Section 2.1. Subsequently, the optimal solution of \hat{x}_t has the form of (16).

9.3 Proof of Proposition 1

Before moving on, two useful lemmas are introduced.

Lemma 2 [18, Lemma 1], [19, Lemma 1] For any two matrices $\Psi = [\psi^1, \psi^2, \dots, \psi^N] \in \mathbb{R}^{n_1 \times N}$ and $\Phi = [\phi^1, \phi^2, \dots, \phi^N] \in \mathbb{R}^{n_2 \times N}$ with i.i.d elements $\psi^i \sim \mathcal{N}(0, \sigma_{\psi}^2 I_{n_1})$ and $\phi^i \sim \mathcal{N}(0, \sigma_{\phi}^2 I_{n_2})$, $i = 1, \dots, N$,

$$\|\Psi\Phi^T\|_2 \leq 4\sigma_{\psi}\sigma_{\phi}\sqrt{N(n_1 + n_2)\log(9/\delta)},$$

holds with probability at least $1 - \delta$ when $N \geq 2(n_1 + n_2)\log(1/\delta)$.

Lemma 3 [18, Lemma 2], [19, Lemma 2] For any matrix $\Psi = [\psi^1, \psi^2, \dots, \psi^N] \in \mathbb{R}^{n \times N}$ with i.i.d elements $\psi^i \sim \mathcal{N}(0, \sigma^2 I_n)$, $i = 1, \dots, N$,

$$\sqrt{\lambda_{\min}(\Psi\Psi^T)} \geq \sigma(\sqrt{N} - \sqrt{n} - \sqrt{2\log(1/\delta)}),$$

holds with probability at least $1 - \delta$.

Then, according to (21), it can be directly derived that

$$\begin{aligned} \|e_Z\|_2 &\leq \left(\left\| G_{\#} \begin{bmatrix} \bar{X}_0 \\ U \end{bmatrix}^T \right\|_2 + \left\| H_{\#} \begin{bmatrix} \bar{X}_0 \\ U \end{bmatrix}^T \right\|_2 \right. \\ & \left. + \left\| V \begin{bmatrix} \bar{X}_0 \\ U \end{bmatrix}^T \right\|_2 \right) \left\| \left(\begin{bmatrix} \bar{X}_0 \\ U \end{bmatrix} \begin{bmatrix} \bar{X}_0 \\ U \end{bmatrix}^T \right)^{-1} \right\|_2. \end{aligned} \quad (38)$$

In the following, the four terms on the right side of (38) are analyzed. For the first term, with probability at least $1 - \delta/4$,

$$\begin{aligned} \left\| G \Xi \begin{bmatrix} \bar{X}_0 \\ U \end{bmatrix}^T \right\|_2 &\leq \rho(G) \left\| \Xi \begin{bmatrix} \bar{X}_0 \\ U \end{bmatrix}^T \right\|_2 \\ &\leq 4\rho(G)\sigma_\xi\sigma_{\max} \sqrt{N(2n + Lm)\log(36/\delta)}, \end{aligned}$$

where the second “ \leq ” is derived using Lemma 2 with Ξ and $[\bar{X}_0^T, U^T]^T$ corresponding to Ψ and Φ , respectively, and $\sigma_{\max} = \max\{\sigma_{\bar{x}_0}, \sigma_u\}$, when $N \geq 2(2n + Lm)\log(4/\delta)$. Similarly, the second term satisfies

$$\begin{aligned} \left\| H \Omega \begin{bmatrix} \bar{X}_0 \\ U \end{bmatrix}^T \right\|_2 &\leq \rho(H) \left\| \Omega \begin{bmatrix} \bar{X}_0 \\ U \end{bmatrix}^T \right\|_2 \\ &\leq 4\rho(H)\sigma_\omega\sigma_{\max} \sqrt{N(n + Ln + Lm)\log(36/\delta)}, \end{aligned}$$

when $N \geq 2(n + Ln + Lm)\log(4/\delta)$. The third term satisfies

$$\begin{aligned} \left\| V \begin{bmatrix} \bar{X}_0 \\ U \end{bmatrix}^T \right\|_2 \\ &\leq 4\sigma_\nu\sigma_{\max} \sqrt{N(n + p + Lp + Lm)\log(36/\delta)}, \end{aligned}$$

with probability at least $1 - \delta/4$ when $N \geq 2(n + p + Lp + Lm)\log(4/\delta)$. By applying Lemma 3, with probability at least $1 - \delta/4$,

$$\begin{aligned} &\sqrt{\lambda_{\min} \left(\begin{bmatrix} \bar{X}_0 \\ U \end{bmatrix} \begin{bmatrix} \bar{X}_0 \\ U \end{bmatrix}^T \right)} \\ &\geq \sigma_{\min} \left(\sqrt{N} - \sqrt{n + Lm} - \sqrt{2\log(4/\delta)} \right) \\ &\geq \frac{1}{2} \sigma_{\min} \sqrt{N}, \end{aligned}$$

where $\sigma_{\min} = \min\{\sigma_{\bar{x}_0}, \sigma_u\}$, and the second “ \geq ” holds when $N \geq 8(n + Lm) + 16\log(4/\delta)$. Hence, the last term on the right side of (38) can be relaxed as

$$\left\| \left(\begin{bmatrix} \bar{X}_0 \\ U \end{bmatrix} \begin{bmatrix} \bar{X}_0 \\ U \end{bmatrix}^T \right)^{-1} \right\|_2 \leq \frac{4}{N\sigma_{\min}^2}.$$

Using the union bound, with probability at least $1 - \delta$,

$$\|e_Z\|_2 < M_Z \sqrt{\frac{\log(36/\delta)}{N}},$$

when $N \geq 8(n + Lm) + 2(Lp + Lm + Ln + p + n + 3)\log(4/\delta)$, where M_Z is a constant defined below (23), and Assumption 2 is used such that $2n + Lm \leq L(2 + m)$,

$n + Ln + Lm < L(1 + n + m)$ and $n + p + Lp + Lm < L(1 + 2p + m)$. Now, the proof of Proposition 1 is complete.

9.4 Proof of Proposition 2

First, note that

$$\begin{aligned} &G_1^T G_1 - G_{1,\#}^T G_{1,\#} \\ &= G_1^T G_1 - G_{1,\#}^T G_1 + G_{1,\#}^T G_1 - G_{1,\#}^T G_{1,\#} \\ &= (G_1 - G_{1,\#})^T G_1 + G_{1,\#}^T (G_1 - G_{1,\#}) \\ &= (G_1 - G_{1,\#})^T G_1 + [(G_{1,\#} - G_1) + G_1]^T (G_1 - G_{1,\#}) \\ &\leq \|G_1 - G_{1,\#}\|_2 \|G_1\|_2 I_n + (\|G_{1,\#} - G_1\|_2 + \|G_1\|_2) \\ &\quad \times \|G_{1,\#} - G_1\|_2 I_n. \end{aligned}$$

Then, it follows from Corollary 1 that, with probability at least $1 - \delta$,

$$G_1^T G_1 - G_{1,\#}^T G_{1,\#} \leq \epsilon_G^2 I_n + 2\epsilon_G \|G_1\|_2 I_n,$$

when $N \geq N_G(\epsilon_G, \delta)$. Further,

$$\begin{aligned} \lambda_{\min}(G_1^T G_1) I_n &\leq G_1^T G_1 = G_1^T G_1 - G_{1,\#}^T G_{1,\#} + G_{1,\#}^T G_{1,\#} \\ &\leq \epsilon_G^2 I_n + 2\epsilon_G \|G_1\|_2 I_n + G_{1,\#}^T G_{1,\#}. \end{aligned}$$

Besides, according to [37, Theorem 6.DO1], $G_1^T G_1 > 0$ when Assumptions 1 and 2 hold, which indicates $\lambda_{\min}(G_1^T G_1) > 0$ always holds. All together, with probability at least $1 - \delta$,

$$G_{1,\#}^T G_{1,\#} \geq \left[\lambda_{\min}(G_1^T G_1) - \epsilon_G^2 - 2\epsilon_G \|G_1\|_2 \right] I_n > 0,$$

when $N \geq N_G(\epsilon_G, \delta)$ and $\epsilon_G < \sqrt{\|G_1\|_2^2 + \lambda_{\min}(G_1^T G_1)} - \|G_1\|_2$. This ensures that $G_{1,\#}$ has full column rank.

9.5 Proof of Proposition 3

From (11) and (15a), we have

$$\begin{aligned} A - A_\# &= G_1^\dagger G_2 - G_{1,\#}^\dagger G_{2,\#} \\ &= G_1^\dagger G_2 - G_{1,\#}^\dagger G_2 + G_{1,\#}^\dagger G_2 - G_{1,\#}^\dagger G_{2,\#} \\ &= (G_1^\dagger - G_{1,\#}^\dagger) G_1 A + G_{1,\#}^\dagger (G_2 - G_{2,\#}) \\ &= G_{1,\#}^\dagger (G_{1,\#} - G_1) A + G_{1,\#}^\dagger (G_2 - G_{2,\#}), \end{aligned}$$

where the last “=” is based on $G_{1,\#}^\dagger G_{1,\#} = G_1^\dagger G_1 = I_n$. According to the results revealed in Corollary 1, with probability at least $1 - \delta$,

$$\|A - A_\#\|_2 \leq \|G_{1,\#}^\dagger\|_2 \left(\|A\|_2 + 1 \right) \epsilon_G,$$

when $N \geq N_G(\epsilon_G, \delta)$ with $\epsilon_G < \epsilon_0$ in (23). Since $G_{1,\#}^\dagger = (G_{1,\#}^T G_{1,\#})^{-1} G_{1,\#}^T$, we have

$$\begin{aligned} \|G_{1,\#}^\dagger\|_2 &= \sqrt{\lambda_{\max}((G_{1,\#}^\dagger)^T G_{1,\#}^\dagger)} = \sqrt{\lambda_{\max}(G_{1,\#}^\dagger (G_{1,\#}^\dagger)^T)} \\ &= \sqrt{\lambda_{\max}((G_{1,\#}^T G_{1,\#})^{-1})} = \sqrt{1/\lambda_{\min}(G_{1,\#}^T G_{1,\#})} \\ &\leq \sqrt{\frac{1}{\lambda_{\min}(G_1^T G_1) - \epsilon_G^2 - 2\epsilon_G \|G_1\|_2}}. \end{aligned}$$

Hence, $\|A\|_2 \|G_{1,\#}^\dagger\|_2 + \|G_{1,\#}^\dagger\|_2$ is uniformly bounded. Therefore, with probability at least $1 - \delta$,

$$\|A - A_\# \|_2 \leq \frac{\|A\|_2 + 1}{\sqrt{\lambda_{\min}(G_1^T G_1) - \epsilon_G^2 - 2\epsilon_G \|G_1\|_2}} \epsilon_G,$$

when $N \geq N_G(\epsilon_G, \delta)$ with $\epsilon_G < \epsilon_0$. Similarly, with probability at least $1 - \delta$,

$$\|B - B_\# \|_2 \leq \frac{\|B\|_2 + 1}{\sqrt{\lambda_{\min}(G_1^T G_1) - \epsilon_G^2 - 2\epsilon_G \|G_1\|_2}} \epsilon_G,$$

and

$$\|C - C_\# \|_2 \leq \|G_1 - G_{1,\#}\|_2 \leq \epsilon_G.$$

According to the union bound and (23), Proposition 3 is proved.

9.6 Proof of Proposition 4

Note that $P_\#$ and P in (27) and (28) can be rewritten as

$$\begin{aligned} P^{-1} &= (\bar{P}^{-1} + C^T R^{-1} C)^{-1}, \\ P_\#^{-1} &= (\bar{P}_\#^{-1} + C^T R^{-1} C)^{-1}. \end{aligned}$$

Then, it follows from (27) and (28) that

$$\begin{aligned} \bar{P}_\# - \bar{P} & \tag{39} \\ &= A_\# (\bar{P}_\#^{-1} + C^T R^{-1} C)^{-1} A_\# - A (\bar{P}^{-1} + C^T R^{-1} C)^{-1} A \\ &= A_\# (\bar{P}_\#^{-1} + C^T R^{-1} C)^{-1} A_\# - A_\# (\bar{P}_\#^{-1} + C^T R^{-1} C)^{-1} A \\ &\quad + A_\# (\bar{P}^{-1} + C^T R^{-1} C)^{-1} A - A (\bar{P}^{-1} + C^T R^{-1} C)^{-1} A \\ &\quad + A_\# (\bar{P}_\#^{-1} + C^T R^{-1} C)^{-1} A - A_\# (\bar{P}^{-1} + C^T R^{-1} C)^{-1} A. \end{aligned}$$

The first four terms on the right side of the second “=” in (39) satisfy

$$\begin{aligned} & A_\# (\bar{P}_\#^{-1} + C^T R^{-1} C)^{-1} A_\# - A_\# (\bar{P}_\#^{-1} + C^T R^{-1} C)^{-1} A \\ & \quad + A_\# (\bar{P}^{-1} + C^T R^{-1} C)^{-1} A - A (\bar{P}^{-1} + C^T R^{-1} C)^{-1} A \\ &= A_\# (\bar{P}_\#^{-1} + C^T R^{-1} C)^{-1} (A_\# - A) \\ & \quad + (A_\# - A) (\bar{P}_\#^{-1} + C^T R^{-1} C)^{-1} A \\ &\leq \|A_\# (\bar{P}_\#^{-1} + C^T R^{-1} C)^{-1}\|_2 \|A_\# - A\|_2 I_n \\ & \quad + \|(\bar{P}_\#^{-1} + C^T R^{-1} C)^{-1} A\|_2 \|A_\# - A\|_2 I_n \\ &\leq M_1 \epsilon I_n, \end{aligned}$$

with probability at least $1 - \delta$, where $M_1 \triangleq \|A_\# (\bar{P}_\#^{-1} + C^T R C)^{-1}\|_2 + \|(\bar{P}_\#^{-1} + C^T R C)^{-1} A\|_2$, when $N \geq N_0(\epsilon, \delta)$ and $\epsilon < \epsilon_0$. For the last two terms in (39), we have

$$\begin{aligned} & A_\# \left((\bar{P}_\#^{-1} + C^T R^{-1} C)^{-1} - (\bar{P}^{-1} + C^T R^{-1} C)^{-1} \right) A \\ &= A_\# (\bar{P}_\#^{-1} + C^T R^{-1} C)^{-1} \left((\bar{P}^{-1} + C^T R^{-1} C) \right. \\ & \quad \left. - (\bar{P}_\#^{-1} + C^T R^{-1} C) \right) (\bar{P}^{-1} + C^T R^{-1} C)^{-1} A_\# \\ &= A_\# (\bar{P}_\#^{-1} + C^T R^{-1} C)^{-1} (\bar{P}^{-1} - \bar{P}_\#^{-1}) \\ & \quad \times (\bar{P}^{-1} + C^T R^{-1} C)^{-1} A \\ &= A_\# (\bar{P}_\#^{-1} + C^T R^{-1} C)^{-1} \bar{P}_\#^{-1} (\bar{P}_\# - \bar{P}) \bar{P}^{-1} \\ & \quad \times (\bar{P}^{-1} + C^T R^{-1} C)^{-1} A. \end{aligned}$$

By denoting

$$\tilde{A}_\# = A_\# (\bar{P}_\#^{-1} + C^T R^{-1} C)^{-1} \bar{P}_\#^{-1},$$

and

$$\tilde{A} = A (\bar{P}^{-1} + C^T R^{-1} C)^{-1} \bar{P}^{-1},$$

we have that $\bar{P}_\# - \bar{P}$ in (39) satisfies

$$\begin{aligned} \bar{P}_\# - \bar{P} &\leq M_1 \epsilon I_n + \tilde{A}_\# (\bar{P}_\# - \bar{P}) \tilde{A}^T \\ &\leq M_1 \epsilon I_n + M_1 \epsilon \tilde{A}_\# \tilde{A}^T + \tilde{A}_\#^2 (\bar{P}_\# - \bar{P}) (\tilde{A}^T)^2 \\ &\quad \vdots \\ &\leq M_1 \epsilon \sum_{h=0}^{\infty} \tilde{A}_\#^h (\tilde{A}^T)^h + \tilde{A}_\#^\infty (\bar{P}_\# - \bar{P}) (\tilde{A}^T)^\infty. \end{aligned} \tag{40}$$

To proceed, by expanding

$$(\bar{P}^{-1} + C^T R^{-1} C)^{-1} = \bar{P} - \bar{P} C^T (R + C \bar{P} C^T) C \bar{P},$$

we can find that

$$\tilde{A} = A - A \bar{P} C^T (R + C \bar{P} C^T) C = A (I_n - L_\infty C),$$

is a closed-loop state matrix and Schur stable. Similarly, $\tilde{A}_\#$ is Schur stable. Hence, we have $\tilde{A}_\#^\infty(\tilde{P}_\# - \bar{P})(\tilde{A}^T)^\infty = 0$ in (40) and

$$\tilde{P}_\# - \bar{P} \leq M_1 \epsilon \sum_{h=0}^{\infty} \tilde{A}_\#^h (\tilde{A}^T)^h.$$

According to [42, Lemma 3, Theorem 2], there exists a positive constant M_2 such that $\sum_{h=0}^{\infty} \tilde{A}_\#^h (\tilde{A}^T)^h \leq M_2 I_n$, which leads to

$$\tilde{P}_\# - \bar{P} \leq M_1 M_2 \epsilon I_n.$$

Note that

$$\epsilon \sim \mathcal{O}\left(\sqrt{\frac{\log(1/\delta)}{N}}\right),$$

when $N \geq N_0(\epsilon, \delta)$ and $\epsilon < \epsilon_0$. Now, combining the above results concludes the proof of the first inequality in Proposition 4. Similarly, the second one can be proved.

9.7 Proof of Theorem 1

First of all, it follows from (1) and (16) that

$$e_{k+1} = (I_n - L^\# C) A_\# e_k + (I_n - L^\# C)(A_\# - A)x_k - (I_n - L^\# C)\omega_k + L^\# \nu_{k+1}.$$

Then, its covariance satisfies

$$\begin{aligned} P_{e,k+1} &= (I_n - L^\# C) A_\# \mathbb{E}\{e_k e_k^T\} A_\#^T (I_n - L^\# C)^T \\ &+ (I_n - L^\# C) A_\# \mathbb{E}\{e_k x_k^T\} (A_\# - A)^T (I_n - L^\# C)^T \\ &+ (I_n - L^\# C)(A_\# - A) \mathbb{E}\{x_k e_k^T\} A_\#^T (I_n - L^\# C)^T \\ &+ (I_n - L^\# C)(A_\# - A) \mathbb{E}\{x_k x_k^T\} (A_\# - A)^T (I_n - L^\# C)^T \\ &+ (I_n - L^\# C) Q (I_n - L^\# C)^T + L^\# R (L^\#)^T \\ &\leq (1 + \eta)(I_n - L^\# C) A_\# P_{e,k} A_\#^T (I_n - L^\# C)^T + L^\# R (L^\#)^T \\ &+ (1 + 1/\eta)(I_n - L^\# C)(A_\# - A) \mathbb{E}\{x_k x_k^T\} (A_\# - A)^T \\ &\times (I_n - L^\# C)^T + (I_n - L^\# C) Q (I_n - L^\# C)^T, \end{aligned}$$

where $\eta < \min\{\|A_\# - A\|_2, 1/|\lambda((I_n - L^\# C)A_\#)|^2 - 1\}$ and “ \leq ” is based on that $AB^T + BA^T \leq \eta AA^T + 1/\eta BB^T$ holds for any square matrices A and B , and any positive scalar η . According to Assumption 4, we further have

$$P_{e,k+1} \leq (1 + \eta)(I_n - L^\# C) A_\# P_{e,k} A_\#^T (I_n - L^\# C)^T + M_3,$$

where

$$M_3 = (1 + 1/\eta)(I_n - L^\# C)(A_\# - A)\Pi(A_\# - A)^T \times (I_n - L^\# C)^T + (I_n - L^\# C)Q(I_n - L^\# C)^T + L^\# R(L^\#)^T,$$

is a constant matrix. Due to $\eta < \min\{1/|\lambda((I_n - L^\# C)A_\#)|^2 - 1\}$, we can find that $\sqrt{1 + \eta}(I_n - L^\# C)A_\#$ is Schur stable since $(I_n - L^\# C)A_\#$ is Schur stable. Hence, the above inequality can guarantee that $P_{e,k+1}$ is uniformly bounded. Next, the error between $P_{e,k}$ and $P_\#$ in (27) is analyzed. According to the above inequality and (27), we can derive that

$$P_{e,k+1} - P_\# \leq (I_n - L^\# C) A_\# (P_{e,k} - P_\#) A_\#^T (I_n - L^\# C)^T + M_4 \|A_\# - A\|_2 I_n,$$

where M_4 is a positive constant scalar. Subsequently,

$$\begin{aligned} &P_{e,k+1} - P_\# \\ &\leq ((I_n - L^\# C) A_\#)^{k+1} (P_{e,0} - P_\#) (A_\#^T (I_n - L^\# C)^T)^{k+1} \\ &+ \|A_\# - A\|_2 \sum_{h=0}^k M_4 ((I_n - L^\# C) A_\#)^h (A_\#^T (I_n - L^\# C)^T)^h, \end{aligned}$$

When k tends to infinity, we have

$$P_{e,\infty} - P_\# \leq M_5 \|A_\# - A\|_2,$$

where

$$M_5 = M_4 \sum_{h=0}^{\infty} ((I_n - L^\# C) A_\#)^h (A_\#^T (I_n - L^\# C)^T)^h,$$

is a constant matrix according to [42, Lemma 3, Theorem 2]. With the results in Propositions 3 and 4, using the union bound, there exists a positive constant M_e that

$$\begin{aligned} \|P_{e,\infty} - P\|_2 &\leq \|P_{e,\infty} - P_\#\|_2 + \|P - P_\#\|_2 \\ &\leq M_e \epsilon \sim \mathcal{O}\left(\sqrt{\frac{\log(1/\delta)}{N}}\right), \end{aligned}$$

with probability at least $1 - 2\delta$, when $N \geq N_0(\epsilon, \delta)$ in (26) with $\epsilon < \epsilon_0$. Thus, the proof of Theorem 1 is complete.

9.8 Proof of Theorem 2

First, we prove that $A_\# + B_\# K_s C_\#$ is Schur stable when the conditions in Theorem 2 hold. It suffices to prove that there exist two positive definite matrices P_K and Δ such that

$$(A_\# + B_\# K_s C_\#) P_K (A_\# + B_\# K_s C_\#)^T - P_K < -\Delta.$$

Let $Q_K = [Q_1^T, Q_2^T]^T \triangleq [I_n, (K_s C_\#)^T]^T P_K$. The above Lyapunov function can be re-written as

$$[A_\# \ B_\#] Q_K P_K^{-1} Q_K^T [A_\#^T \ B_\#^T]^T - P_K < -\Delta.$$

By using Schur complement and substituting the expressions of $A_{\#}$, $B_{\#}$ and $C_{\#}$ in (15) into the above inequality, it is equivalent to (31). This is, $A_{\#} + B_{\#}K_sC_{\#}$ is Schur stable when K_s is any solution to $K_sG_{4,\#}Q_1 = Q_2$ and (31) is satisfied.

Next, it is proved that $A + BK_sC$ is Schur stable. It follows from Proposition 3 that

$$\begin{aligned} & \|A + BK_sC - (A_{\#} + B_{\#}K_sC_{\#})\|_2 \\ & \leq \|A - A_{\#}\|_2 + \|BK_s\|_2\|C - C_{\#}\|_2 + \|B - B_{\#}\|_2\|K_sC_{\#}\|_2 \\ & \leq \epsilon(1 + \|B_{\#}K_s\|_2 + \epsilon\|K_s\|_2 + \|K_sC_{\#}\|_2) \triangleq \epsilon M_K, \end{aligned}$$

with probability at least $1 - \delta$, when $N \geq N_0(\epsilon, \delta)$ and $\epsilon < \epsilon_0$. Further, we have

$$\begin{aligned} & (A + BK_sC)P_K(A + BK_sC)^T - P_K \\ & = ((A + BK_sC) - (A_{\#} + B_{\#}K_sC_{\#}))P_K(A + BK_sC)^T \\ & \quad + (A_{\#} + B_{\#}K_sC_{\#})P_K((A + BK_sC) - (A_{\#} + B_{\#}K_sC_{\#}))^T \\ & \quad + (A_{\#} + B_{\#}K_sC_{\#})P_K(A_{\#} + B_{\#}K_sC_{\#})^T - P_K \\ & \leq \epsilon M_K(2\|(A_{\#} + B_{\#}K_sC_{\#})Q_1\|_2 + \epsilon_0 M_K\|Q_1\|_2)I_n - \Delta. \end{aligned}$$

Hence, when $\epsilon \leq \epsilon_1$ with

$$\epsilon_1 = \frac{\lambda_{\min}(\Delta)}{M_K(2\|(A_{\#} + B_{\#}K_sC_{\#})Q_1\|_2 + \epsilon_0 M_K\|Q_1\|_2)}, \quad (41)$$

we have

$$(A + BK_sC)P_K(A + BK_sC)^T - P_K < 0,$$

which indicates that $A + BK_sC$ is Schur stable.

9.9 Proof of Theorem 3

First of all, denote $\check{x}_k = [x_k^T, e_k^T]^T$. According to (1), (16) and (32), the dynamics of \check{x}_k can be derived

$$\check{x}_{k+1} = \check{A}\check{x}_k + \begin{bmatrix} I_n \\ L^{\#}C - I_n \end{bmatrix} \omega_k + \begin{bmatrix} 0 \\ L^{\#} \end{bmatrix} \nu_{k+1}.$$

where $\check{A} = \check{A}_1 + \check{A}_2$ with

$$\check{A}_1 = \begin{bmatrix} A + BK_d & BK_d \\ 0 & (I_n - L^{\#}C)A_{\#} \end{bmatrix},$$

and

$$\check{A}_2 = \begin{bmatrix} 0 & 0 \\ (I_n - L^{\#}C)(A_{\#} - A) & 0 \end{bmatrix}.$$

To ensure the stability, it suffices to prove that \check{A} is Schur stable. By referring to the proofs of Theorems 1 and 2, we have that $A + BK_d$ and $(I_n - L^{\#}C)A_{\#}$ are simultaneously Schur stable with probability at least $1 - \delta$, when $N \geq N_0(\epsilon, \delta)$ with $\epsilon < \min\{\epsilon_0, \epsilon_1\}$. This ensures that \check{A}_1 is Schur stable. Hence, we can find a positive definite matrix $P_{\check{A}}$ that

$$\check{A}_1 P_{\check{A}} \check{A}_1^T - P_{\check{A}} < 0.$$

From Proposition 3, we have

$$\begin{aligned} & (\check{A}_1 + \check{A}_2)P_{\check{A}}(\check{A}_1 + \check{A}_2)^T - P_{\check{A}} - (\check{A}_1 P_{\check{A}} \check{A}_1^T - P_{\check{A}}) \\ & \leq \epsilon\|I_n - L^{\#}C\|_2\|P_{\check{A}}\|_2(2\|\check{A}_1\|_2 + \epsilon\|I_n - L^{\#}C\|_2). \end{aligned}$$

Further, when $\epsilon < \epsilon_2$ with

$$\epsilon_2 = \frac{\lambda_{\min}(P_{\check{A}} - \check{A}_1 P_{\check{A}} \check{A}_1^T)}{\|I_n - L^{\#}C\|_2\|P_{\check{A}}\|_2(2\|\check{A}_1\|_2 + \epsilon_0\|I_n - L^{\#}C\|_2)}, \quad (42)$$

we have

$$(\check{A}_1 + \check{A}_2)P_{\check{A}}(\check{A}_1 + \check{A}_2)^T - P_{\check{A}} < 0.$$

That is, \check{A} is Schur stable. Now, the proof of Theorem 3 is complete.

References

- [1] R. E. Kalman, "A new approach to linear filtering and prediction problems," *Transaction of the ASME-Journal of Basic Engineering*, pp. 35–45.
- [2] F. Auger, M. Hilaret, J. M. Guerrero, E. Monmasson, T. Orłowska-Kowalska, and S. Katsura, "Industrial applications of the Kalman filter: A review," *IEEE Transactions on Industrial Electronics*, vol. 60, no. 12, pp. 5458–5471, 2013.
- [3] O. Chutatape, L. Zheng, and S. M. Krishnan, "Retinal blood vessel detection and tracking by matched Gaussian and Kalman filters," in *Proceedings of the 20th Annual International Conference of the IEEE Engineering in Medicine and Biology Society*, pp. 3144–3149, 1998.
- [4] F. Cassola and M. Burlando, "Wind speed and wind energy forecast through Kalman filtering of numerical weather prediction model output," *Applied Energy*, vol. 99, pp. 154–166, 2012.
- [5] B. D. Anderson and J. B. Moore, *Optimal Filtering*. Mineola, N.Y: Dover Publications, 2005.
- [6] M. Verhaegen and V. Verdult, *Filtering and System Identification: A Least Squares Approach*. Cambridge University Press, 2007.
- [7] A. Carron, M. Todescato, R. Carli, L. Schenato, and G. Pillonetto, "Machine learning meets Kalman filtering," in *IEEE 55th Conference on Decision and Control*, pp. 4594–4599, 2016.

- [8] Z.-S. Hou and Z. Wang, "From model-based control to data-driven control: Survey, classification and perspective," *Information Sciences*, vol. 235, pp. 3–35, 2013.
- [9] K. J. Åström and B. Wittenmark, *Adaptive Control*. MA: Addison-Wesley, 1995.
- [10] S. G. Khan, G. Herrmann, F. L. Lewis, T. Pipe, and C. Melhuish, "Reinforcement learning and optimal adaptive control: An overview and implementation examples," *Annual Reviews in Control*, vol. 36, no. 1, pp. 42–59, 2012.
- [11] M. O. Williams, I. G. Kevrekidis, and C. W. Rowley, "A data-driven approximation of the Koopman operator: Extending dynamic mode decomposition," *Journal of Nonlinear Science*, vol. 25, pp. 1307–1346, 2015.
- [12] C. De Persis and P. Tesi, "Formulas for data-driven control: Stabilization, optimality, and robustness," *IEEE Transactions on Automatic Control*, vol. 65, no. 3, pp. 909–924, 2019.
- [13] C. De Persis and P. Tesi, "Low-complexity learning of linear quadratic regulators from noisy data," *Automatica*, vol. 128, p. 109548, 2021.
- [14] H. J. Van Waarde, J. Eising, H. L. Trentelman, and M. K. Camlibel, "Data informativity: A new perspective on data-driven analysis and control," *IEEE Transactions on Automatic Control*, vol. 65, no. 11, pp. 4753–4768, 2020.
- [15] J. Coulson, J. Lygeros, and F. Dörfler, "Data-enabled predictive control: In the shallows of the DeePC," in *18th European Control Conference*, pp. 307–312, 2019.
- [16] J. Berberich, J. Köhler, M. A. Müller, and F. Allgöwer, "Data-driven model predictive control with stability and robustness guarantees," *IEEE Transactions on Automatic Control*, vol. 66, no. 4, pp. 1702–1717, 2020.
- [17] S. Oymak and N. Ozay, "Non-asymptotic identification of LTI systems from a single trajectory," in *2019 American control conference*, pp. 5655–5661, 2019.
- [18] S. Dean, H. Mania, N. Matni, B. Recht, and S. Tu, "On the sample complexity of the linear quadratic regulator," *Foundations of Computational Mathematics*, vol. 20, no. 4, pp. 633–679, 2020.
- [19] Y. Zheng and N. Li, "Non-asymptotic identification of linear dynamical systems using multiple trajectories," *IEEE Control Systems Letters*, vol. 5, no. 5, pp. 1693–1698, 2020.
- [20] Y. Zheng, L. Furieri, M. Kamgarpour, and N. Li, "Sample complexity of linear quadratic Gaussian (LQG) control for output feedback systems," in *Proceedings of Machine Learning Research*, pp. 559–570, PMLR, 2021.
- [21] R. Mehra, "On the identification of variances and adaptive Kalman filtering," *IEEE Transactions on Automatic Control*, vol. 15, no. 2, pp. 175–184, 1970.
- [22] S. Shafieezadeh Abadeh, V. A. Nguyen, D. Kuhn, and P. M. Mohajerin Esfahani, "Wasserstein distributionally robust Kalman filtering," *Advances in Neural Information Processing Systems*, vol. 31, 2018.
- [23] A. Tsiamis and G. J. Pappas, "Finite sample analysis of stochastic system identification," in *IEEE 58th Conference on Decision and Control*, pp. 3648–3654, 2019.
- [24] A. Tsiamis, N. Matni, and G. Pappas, "Sample complexity of Kalman filtering for unknown systems," in *Learning for Dynamics and Control*, pp. 435–444, 2020.
- [25] G. Revach, N. Shlezinger, R. J. Van Sloun, and Y. C. Eldar, "Kalmannet: Data-driven Kalman filtering," in *IEEE International Conference on Acoustics, Speech and Signal Processing*, pp. 3905–3909, 2021.
- [26] G. Revach, N. Shlezinger, X. Ni, A. L. Escoriza, R. J. G. van Sloun, and Y. C. Eldar, "Kalmannet: Neural network aided Kalman filtering for partially known dynamics," *IEEE Transactions on Signal Processing*, vol. 70, pp. 1532–1547, 2022.
- [27] M. Netto and L. Mili, "A robust data-driven Koopman Kalman filter for power systems dynamic state estimation," *IEEE Transactions on Power Systems*, vol. 33, no. 6, pp. 7228–7237, 2018.
- [28] I. Markovskiy, "A missing data approach to data-driven filtering and control," *IEEE Transactions on Automatic Control*, vol. 62, no. 4, pp. 1972–1978, 2017.
- [29] M. I. Jordan and T. M. Mitchell, "Machine learning: Trends, perspectives, and prospects," *Science*, vol. 349, no. 6245, pp. 255–260, 2015.
- [30] Y. Weng, R. Negi, C. Faloutsos, and M. D. Ilić, "Robust data-driven state estimation for smart grid," *IEEE Transactions on Smart Grid*, vol. 8, no. 4, pp. 1956–1967, 2017.
- [31] A. S. Zamzam, X. Fu, and N. D. Sidiropoulos, "Data-driven learning-based optimization for distribution system state estimation," *IEEE Transactions on Power Systems*, vol. 34, no. 6, pp. 4796–4805, 2019.
- [32] T. M. Wolff, V. G. Lopez, and M. A. Müller, "Data-based moving horizon estimation for linear discrete-time systems," in *2022 European Control Conference (ECC)*, pp. 1778–1783, 2022.
- [33] D. Shi, T. Chen, and L. Shi, "Event-triggered maximum likelihood state estimation," *Automatica*, vol. 50, no. 1, pp. 247–254, 2014.
- [34] G. F. Franklin, J. D. Powell, A. Emami-Naeini, and J. D. Powell, *Feedback Control of Dynamic Systems*. Pearson Prentice Hall, 2006.
- [35] H. E. Rauch, F. Tung, and C. T. Striebel, "Maximum likelihood estimates of linear dynamic systems," *Journal of the American Institute of Aeronautics and Astronautics*, vol. 3, no. 8, pp. 1445–1450, 1965.
- [36] G. Goodwin, M. M. Seron, and J. A. De Doná, *Constrained Control and Estimation: An Optimisation Approach*. New York: Springer Science & Business Media, 2005.
- [37] C.-T. Chen, *Linear System Theory and Design*. New York, NY: Oxford University Press, 1984.
- [38] S. Boyd, N. Parikh, E. Chu, B. Peleato, J. Eckstein, et al., "Distributed optimization and statistical learning via the alternating direction method of multipliers," *Foundations and Trends® in Machine Learning*, vol. 3, no. 1, pp. 1–122, 2011.
- [39] L. Ljung, *System Identification: Theory for the User*. Upper Saddle River, USA: PTR Prentice Hall, 1999.
- [40] S. Oymak and N. Ozay, "Revisiting Ho–Kalman-based system identification: Robustness and finite-sample analysis," *IEEE Transactions on Automatic Control*, vol. 67, no. 4, pp. 1914–1928, 2022.
- [41] M. Ruderman, J. Krettek, F. Hoffmann, and T. Bertram, "Optimal state space control of DC motor," *IFAC Proceedings Volumes*, vol. 41, no. 2, pp. 5796–5801, 2008.
- [42] J. Qian, Z. Duan, P. Duan, and Z. Li, "Observation of periodic systems: Bridge centralized Kalman filtering and consensus-based distributed filtering," *IEEE Transactions on Automatic Control*, in press, doi:10.1109/TAC.2023.3290105.